Research paper

Novel quinazolinone inhibitors of the *Pseudomonas aeruginosa* quorum sensing transcriptional regulator PqsR

Scott Grossman [a, 1], Fadi Soukarieh [b, c, 1], William Richardson [a], Ruiling Liu [a], Alaa Mashabi [a], Jonas Emsley [a, c], Paul Williams [b, c], Miguel Cámara [b, c], Michael J. Stocks [a, c, *]

[a] *School of Pharmacy, University of Nottingham Biodiscovery Institute, University Park, Nottingham, Nottinghamshire, NG7 2RD, UK*
[b] *School of Life Sciences, University of Nottingham Biodiscovery Institute, University Park, Nottingham, Nottinghamshire, NG7 2RD, UK*
[c] *National Biofilms Innovation Centre, University of Nottingham Biodiscovery Institute, University Park, Nottingham, Nottinghamshire, NG7 2RD, UK*

A R T I C L E   I N F O

A B S T R A C T

Rising numbers of cases of multidrug- and extensively drug-resistant *Pseudomonas aeruginosa* over recent years have created an urgent need for novel therapeutic approaches to cure potentially fatal infections. One such approach is virulence attenuation where anti-virulence compounds, designed to reduce pathogenicity without affording bactericidal effects, are employed to treat infections. *P. aeruginosa* uses the *pqs* quorum sensing (QS) system, to coordinate the expression of a large number of virulence determinants as well as bacterial-host interactions and hence represents an excellent anti-virulence target.

We report the synthesis and identification of a new series of thiazole-containing quinazolinones capable of inhibiting PqsR, the transcriptional regulator of the *pqs* QS system. The compounds demonstrated high potency ($IC_{50} < 300$ nM) in a whole-cell assay, using a mCTX:P_{pqsA}-*lux*-based bioreporter for the *P. aeruginosa* PAO1-L and PA14 strains. Structural evaluation defined the binding modes of four analogues in the ligand-binding domain of PqsR through X-ray crystallography. Further work showed the ability of 6-chloro-3((2-pentylthiazol-4-yl)methyl)quinazolin-4(3H)-one (**18**) and 6-chloro-3((2-hexylthiazol-4-yl)methyl)quinazolin-4(3H)-one (**19**) to attenuate production of the PqsR-regulated virulence factor pyocyanin. Compounds **18** and **19** showed a low cytotoxic profile in the A549 human epithelial lung cell line making them suitable candidates for further pre-clinical evaluation.

1. Introduction

Pseudomonas aeruginosa (PA), a Gram-negative pathogenic bacterium found widely in nature, is a common cause of infection in immunocompromised patients. Chronic and recurring infections are widespread, and PA infection is frequently associated with respiratory failure, reduced pulmonary function and mortality within cystic fibrosis patients [1–3]. A rise in multidrug resistant cases of PA has raised this organism to a priority class pathogen of critical importance by the World Health Organisation [4].

In order to combat the threat of antimicrobial resistance, novel strategies are required to provide long-lasting solutions, which drastically reduce the rate of emergence of resistance due to the high selective pressure posed by current antibiotic treatments. One such approach is the use of alternative treatments which can attenuate virulence within bacterial populations without directly killing the infectious organisms and/or sensitise these populations to the action of existing antibiotics [5,6]. The net result is a non-pathogenic population which can be cleared by the immune system or which may become sensitive to existing antimicrobials [6–9].

Extensive work associated with this approach has investigated inhibition of quorum sensing systems within bacterial populations. Quorum sensing (QS) is a cell-to-cell communication strategy used by microbes to coordinate the production of numerous traits including virulence factors in a population-dependent manner. QS relies on the production and sensing of small diffusible signal

molecules known as autoinducers (AIs) or QS signal molecules (QSSMs) [10−12]. Although most commonly observed as an intra-species event, QS is also seen at the interspecies and inter-kingdom level through bacteria-bacteria communication systems as well as in bacteria-fungi mixed populations [13−15].

During infection QS in PA controls the production of virulence traits such as the phenazine, pyocyanin and the siderophore pyo-verdine, which are capable of cytotoxic effects against mammalian cells and iron scavenging respectively, as well as those responsible for bacterial motility and biofilm formation [16−22].

PA utilises three closely interlinked QS systems to fully elicit its pathogenicity; the *las* and *rhl* systems which operate *via N*-acylho-moserine lactones as their QSSMs (**1**, **2**), whereas the *pqs* system uses alkylquinolones (AQ), namely 2-heptylquinolin-4(1*H*)-one (HHQ, **3**) and the *Pseudomonas* Quinolone Signal (2-heptyl-3-hydroxy-4(1*H*)-quinolone, PQS, **4**) as their cognate signals (Fig. 1) [7,11,23−25].

The *pqs* QS system of PA requires the *pqsABCDE* operon for the biosynthesis of HHQ **3**, the precursor of PQS **4**, though the *pqsE* gene product is also known to play both a biosynthetic and a key regu-latory role in the regulation of multiple virulence factors [26−31]. HHQ is converted to PQS *via* the monooxygenase PqsH. The expression of the *pqsABCDE* operon is controlled by the LysR-type transcriptional regulator PqsR upon binding its cognate ligands, PQS and HHQ [32,33].

Inhibition of the *pqs* system can result in a reduction in the production of pyocyanin and alkylquinolones as well as many other virulence traits [32,34−37]. As such, PqsR has been validated as a target for the inhibition of the *pqs* system and hence virulence using both *in vitro* assays and *in vivo* in mouse infection models [37].

Herein we report the discovery of a new series of compounds with high potency against PqsR in two different PA strains (PAO1-L and PA14) that represent the two major genomic groups. Binding of compounds **6**, **12**, **18** and **19** to this regulatory protein is shown through co-crystallisation into the ligand-binding domain (LBD) of PqsR [32,36]. The lead compounds (**18**, **19**) were shown to attenuate pyocyanin production and demonstrated very low cytotoxicity against mammalian cells, supporting their suitability for further studies.

2. Results and discussion

2.1. SAR-based design and synthesis of PqsR inhibitors

Previous research has shown that quinazolinone scaffolds can provide the basis for PqsR antagonists, in part due to the similarity this core shares with the endogenous ligands PQS and HHQ [32]. Therefore, it was unsurprising that an *in silico* screen of the

University of Nottingham Managed Chemical Compound Collection (MCCC, a collection of 85,000 diverse compounds) gave several hit compounds bearing this structural motif. One such compound, **5** (Fig. 2), containing a thiazole group proved interesting for further structure activity relationship (SAR) exploration.

Initial testing of **5** showed an activity for PAO1-L of 13.2 ± 2.73 μM in a mCTX-P$_{pqsA}$-*lux* luminescence based bioreporter assay. Further optimisation yielded **6**, with an improved activity of 1.0 ± 0.42 μM. Furthermore, homologous oxadiazole **7** was found to be inactive at 10 μM, providing evidence for the importance of the thiazole ring for inhibiting PqsR. As such, a SAR study was con-ducted around **6**, primarily focussing on 2-substitution of the thiazole.

We envisaged that variation to the isopropyl group of compound **6** was the most promising area to explore with regards to improving potency. A range of alternate functionalities varying from alkyl chains to substituted amines and small aromatic groups provided a diverse set of compounds to explore the space available within the LBD of the PqsR protein where these ligands were believed to bind (Fig. 3).

A four-step synthetic procedure (Scheme 1) provided a robust route to the desired 2,4-disubstituted thiazoles bearing alkyl, amino and aryl functionalities. Initially, 2-amino-5-chlorobenzoic acid was condensed in formamide to give the corresponding 6-chloroquinazolin-4(3*H*)-one **36**. Reaction with chloroacetone gave the intermediate **37**, which was brominated through refluxing in acetic acid with bromine to afford the α-bromoketone **38**. Thiazole formation in ethanol with a range of thioamides gave the 2,4-disubstituted thiazoles **6**, **8−26**.

In addition to this series of 2,4-substituted thiazoles (**6**, **8−26**), a 2,5-substituted thiazole **35** analogous to **6** was synthesised to observe whether altering the orientation of the thiazole ring could improve efficacy, as was purported through a ligand docking screen *in silico*. Furthermore, in a bid to decrease lipophilicity, a range of 2-amino-5-substituted thiazoles were synthesised in a two-step route from 6-chloroquinazolin-4(3*H*)-one (**36**).

Synthesis of the 5-substituted thiazole **35** required an alternate four-step synthetic route (Scheme 2). Initially, bromomalonalde-hyde was condensed with 2-methylpropanethioamide, to give 2-isopropylthiazole-5-carbaldehyde, which was immediately treated with hydroxylamine hydrochloride affording 2-isopropylthiazole-5-carbaldehyde oxime (**39**). Reduction of the oxime using zinc powder and hydrochloric acid gave the primary amine (**40**).

Separately, 2-amino-5-chlorobenzoic acid was treated with DMFDMA to give methyl 5-chloro-2-(((dimethylamino)methylene) amino)benzoate (**41**) [38]. Cyclisation under acidic conditions with

N-butanoyl-L-homoserine lactone **1**

N-(3-oxododecanoyl)-L-homoserine lactone **2**

2-heptylquinolin-4(1*H*)-one **3** (HHQ)

2-heptyl-3-hydroxyquinolin-4(1*H*)-one **4** (PQS)
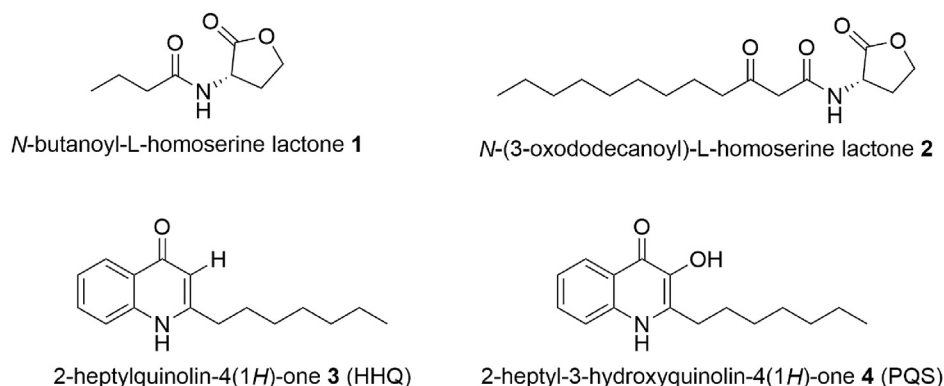
Fig. 1. Known QSSMs in *P. aeruginosa* include *N*-acylhomoserine lactones which regulate **1** the *rhl* and **2** *las* systems, and **3**, **4** HHQ and PQS which regulate the *pqs* system.
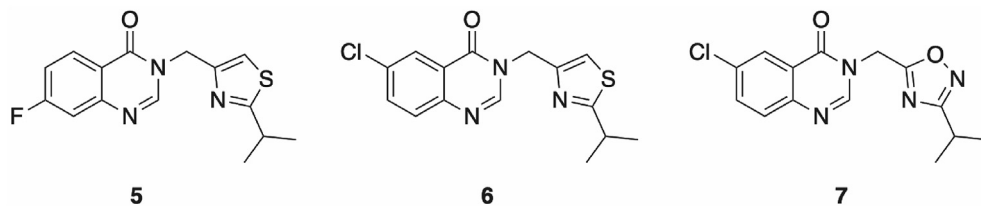
Fig. 2. Hit compound **5** found through *in silico* and subsequent *in vitro* testing of the MCCC compound library, was optimised to yield **6**. Replacing the thiazole moiety with an oxadiazole, as in **7**, yielded an inactive compound when screened at 10 μM ligand concentration.
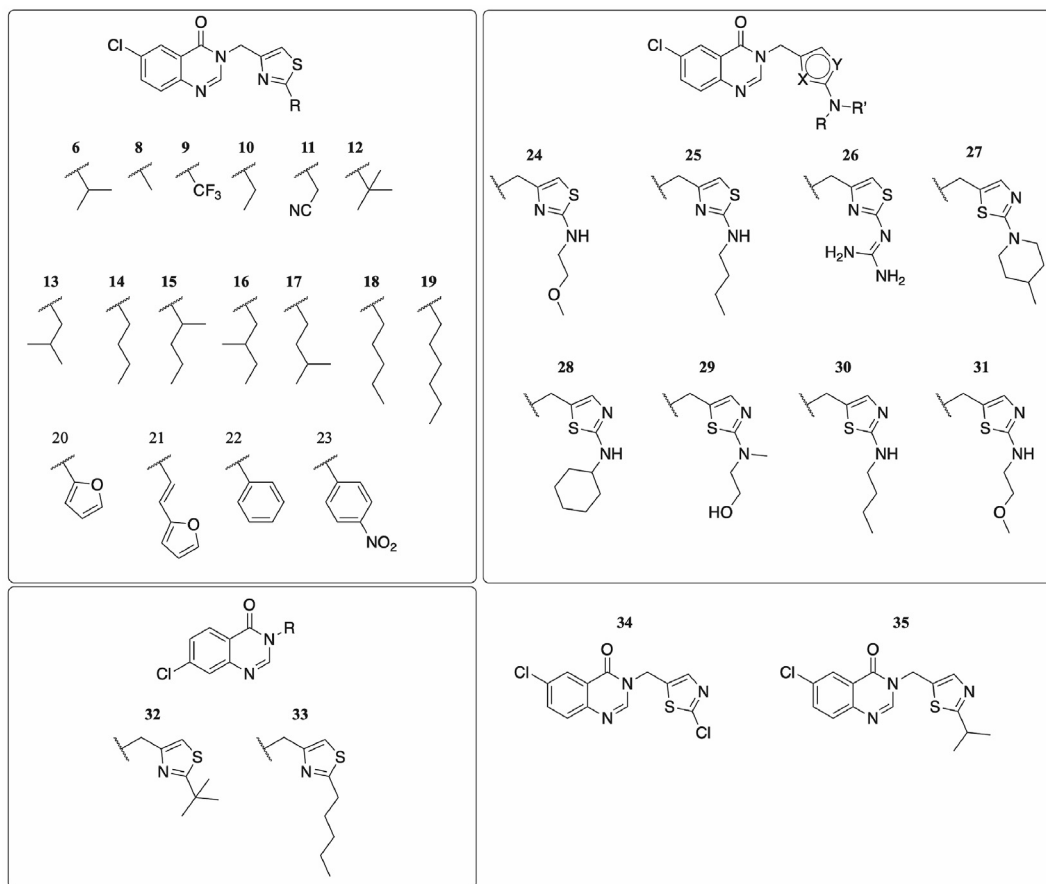
Fig. 3. Structures of all synthesised compounds carried through to *in vitro* testing in PAO1-L.
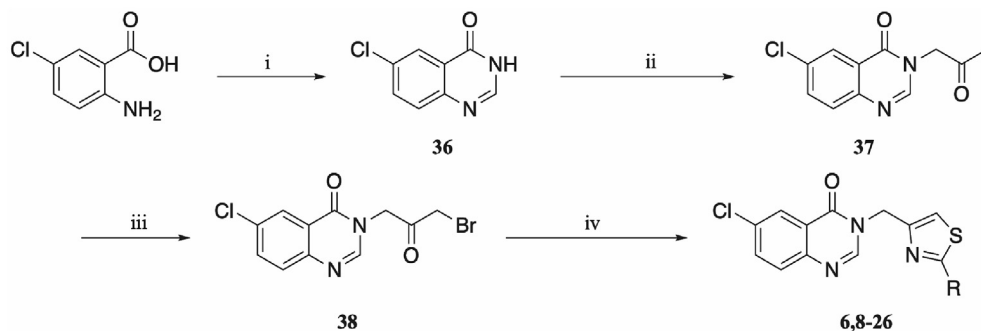
Scheme 1. Synthetic route to compounds **6**, **8**–**26**: (i) formamide, 150 °C, 16 h; (ii) NaH, NMP, 0 °C, 30 min, then chloroacetone, 0 °C, 1 h; (iii) bromine, acetic acid, 65 °C, 16 h; (iv) thioamide or thiourea, ethanol, 80 °C, 16 h; for complete structure of the compounds, see Fig. 3.
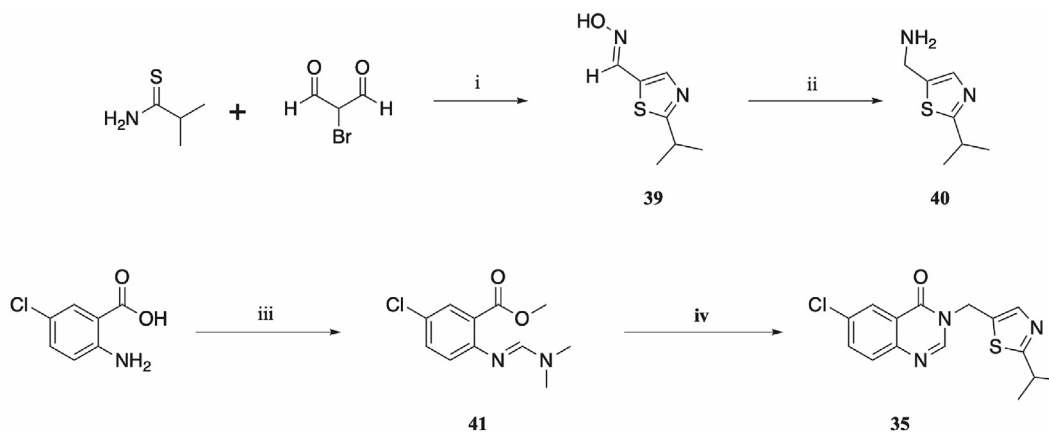
Scheme 2. Synthetic route to **35**: (i) ethanol, rt, 4 h, then NH$_2$OH·HCl, TEA, rt, 2 h; (ii) HCl, zinc powder, 60 °C, 2 h; (iii) DMFDMA, 100 °C, 2 h; (iv) acetic acid, ethanol, 100 °C, 16 h.

methylamino thiazole (**40**) gave the desired product 6-chloro-3-((2-isopropylthiazol-5-yl)methyl)quinazolin-4(3H)-one (**35**).

The 2-amino-5-substituted thiazoles (**27**–**31**) were prepared from reacting 6-chloroquinazolin-4(3H)-one (**36**) with 2-chloro-5-(chloromethyl)thiazole, to give 6-chloro-3-((2-chlorothiazol-5-yl)methyl)quinazolin-4(3H)-one (**34**). Displacement of the chlorine at the 2-position of the thiazole with five different amines under neutral conditions gave products **27**–**31** in yields of 21–84% (Scheme 3).

In addition to variations about the thiazole, changes to the halogen decorating the quinazolinone core could alter binding to PqsR significantly. It was believed that the 6-chloro functionality in **6** could bind into a deep pocket within the LBD of PqsR, and possibly form a hydrogen bond with Thr265, as reported before. However, compounds reported by Ilangovan et al. contained a chlorine at the 7-position of the bicyclic core [32]. Therefore, in order to fully investigate the binding mode of this series, a 7-chloroquinazolin-4(3H)-one subset was synthesised.

Two compounds were synthesised bearing a 7-chloro substitution on the bicyclic ring, with variations on the thiazole: **32** contained a *tert*-butyl group at the thiazole 2-position, and **33** a pentyl chain. The synthetic route was similar to that by which the 6-chloro series was synthesised (Scheme 4), though chlorination of quinazolinone **43** yielded the desired α-haloketone **44**. Subsequent thiazole formation led to the synthesis of **32** and **33**.

2.2. Inhibition of the pqs system by potential PqsR antagonists

A PqsR-dependent bioreporter assay was used to assess the degree to which the compounds synthesised in the SAR study could inhibit the *pqs* QS system. Introduction of a mCTX:P$_{pqsA}$-*lux* transcriptional into the chromosomal CTX sites of PA strains PAO1-L and PA14 results in the production of bioluminescence at high bacterial cell densities in cultures where PQS and HHQ have reached their threshold activation concentrations for PqsR activation and in turn

the P$_{pqsA}$ promoter [39]. Consequently, inhibitors of PqsR reduce bioluminescence levels in these strains. Initially 96-well plates containing the PAO1-L mCTX:P$_{pqsA}$-*lux* bioreporter strain grown in lysogeny broth (LB) were treated with a single concentration of 10 μM of each compound to determine which compounds were active. As a threshold level for compound selection, a 50% reduction of *pqs* activity compared to the DMSO control was set, where *pqs* activity was a ratio of luminescence over OD$_{600}$. Only compounds above the 50% threshold progressed for IC$_{50}$ determination.

Of the 29 compounds tested, 14 compounds showed >50% inhibition at a 10 μM concentration and their concentration-dose response curves were generated. Importantly, the active compounds were found to not inhibit growth compared to the DMSO control (Fig. S2).

From the SAR study, it was apparent that short, unbranched alkyl chains led to a loss of activity, (see compounds **8**–**11**). Furthermore, the addition of heteroatoms into the alkyl chain at the 2-position of the thiazole appeared to reduce activity. Of the seven amino alkyl chain containing compounds, only **25** (IC$_{50}$ = 3.5 μM in PAO1-L) had inhibitory activity at a ligand concentration of 10 μM. The presence of a tertiary amine did not improve activity, and the inclusion of an additional heteroatom led to no inhibition (compound **24**).

Compounds **23** and **26**, both containing three heteroatoms in their side chains, were found to be inactive, further suggesting that increase in polarity in the side chain leads to inactivity. In the case of **23** this may be due to the polarity of the nitro group; its charged state may result in the loss of activity in the whole cell-based assay as a result of poor cell penetration. Compound **26** had the lowest ClogP value of all compounds in the series (1.31). Notably, no compound with a ClogP value under 3.00 showed any activity, which also suggests that difficulty in penetrating the lipid bilayer contributes significantly to the inactivity of these compounds.

For the given series, 6-chloro substitution on the quinazolinone ring demonstrated improved activity over a 7-chloro substituted
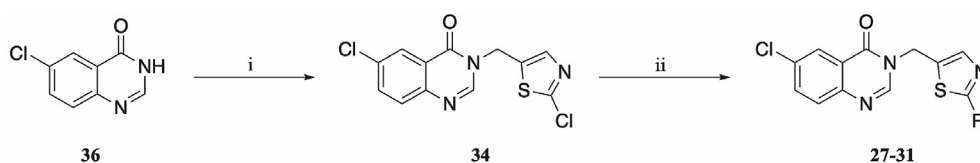
Scheme 3. Synthetic route to **27**–**31**: (i) KOH, TBAI, 2-chloro-5-(chloromethyl)thiazole, toluene, 70 °C, 1 h; (ii) amine, DMSO, 100–130 °C, 16 h; for complete structure of the compounds, see Fig. 3.
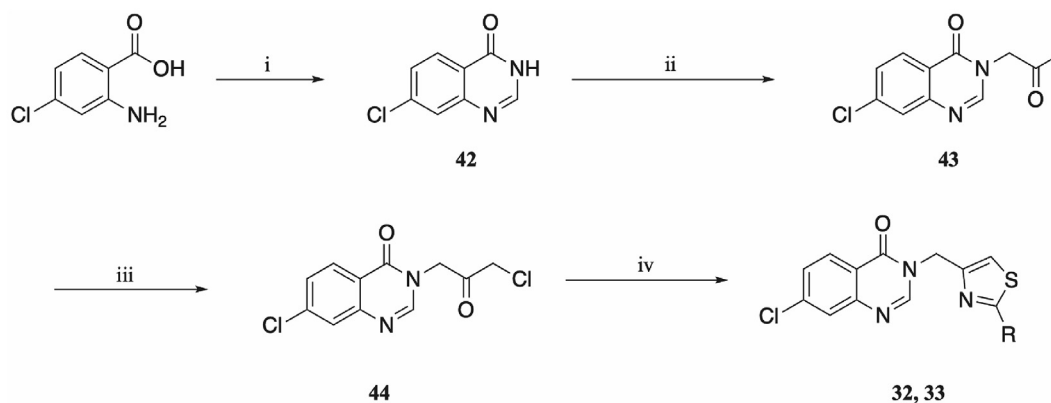
Scheme 4. Synthetic route to **32–34**: (i) formamide, 150 °C, 16 h; (i) NaH, NMP, 0 °C, 30 min, then chloroacetone, 0 °C, 1 h; (iii) NCS, sulfuric acid, DCM, 40 °C, 6 h; (iv) thioamide, acetic acid, ethanol, 80 °C, 16 h; for complete structure of the compounds, see Fig. 3.

scaffold. Compound **32** (IC$_{50}$ = 2.9 μM) was only marginally more active than the lead compound **45** (IC$_{50}$ = 5.0 μM, Fig. 4) of a previously described 7-chloro substituted scaffold [32]. Furthermore, compound **33** was inactive when tested at a ligand concentration of 10 μM. Comparable 6-chloro substituted compounds **12** (IC$_{50}$ = 397 nM) and **18** (IC$_{50}$ = 313 nM) both showed sub-micromolar activity, with **12** displaying seven-fold stronger activity in strain PAO1-L compared with the weakly active **32**.

Moreover, inverting the heteroatoms within the thiazole ring reduced activity, as indicated by the difference in activities of **6** (IC$_{50}$ = 1.0 μM) and **35**; the 2,5- disubstituted thiazole **35** was inactive at a concentration of 10 μM, whereas the 2,4-analogue **6** was previously shown to have an activity of 1.0 μM. This inversion of the thiazole ring may have further contributed to the inactivity of compounds **27–31** in addition to the increased polarity in the side chain.

One argument rationalising the intolerance of heteroatoms may be poor bacterial uptake, or high rates of transporter-based efflux [40]. Although a whole cell approach removes the ability to define a binding event in the context of the assay itself, in combination with X-ray crystallography this methodology allows for definitive selection of compounds which both bind to the desired molecular target, and also have a proven efficacy.

Dose response curves were obtained for all 14 compounds exhibiting >50% inhibition in the 10 μM spot test, with activities ranging from 244 nM to 3.55 μM in the bioreporter strain PAO1-L. Active compounds were then assayed against the clinically-relevant strain PA14 (Table 1). In general, the compounds displayed similar activities in both strains PAO1-L and PA14.

The pharmacological evaluation shed further light on the importance of the 2-substitution of the thiazole. Regarding the length and branching of the alkyl chain, two clear trends became

evident. It was apparent that an increased chain length improved potency, with the two most potent inhibitors bearing a hexyl (**19,** IC$_{50}$ = 298 nM) and pentyl chain (**18**, IC$_{50}$ = 313 nM) respectively. Moreover, increased branching at the 1-position of the alkyl chain greatly improved potency: compound **12** (IC$_{50}$ = 397 nM) containing a *tert*-butyl side chain demonstrated potent activity in strain PAO1-L.

Strain PAO1-L is a moderately virulent laboratory adapted strain routinely used to screen for PqsR inhibitors [34,42]. However, given the genomic diversity of PA strains, it is essential to test isolates belonging to the two major genomic groups. Hence, we also screened the inhibitors against the highly virulent PA14 strain [43]. It was therefore encouraging to see that activities were comparable between these strains. Moreover, for a few select compounds (**15–17, 19, 22**) potencies were shown to be greater in PA14, suggesting broad activity across the two main PA clades.

Three compounds (**18, 19** and **22**, IC$_{50}$ = 244 nM), were selected for X-ray crystallography based on the high potency across both strains. Compound **12** was also chosen for further study, due to its excellent potency in PAO1-L. Furthermore, compound **6** was selected for X-ray crystallography studies to provide a comparison between the first optimised compound in the series, and the most potent compounds.

2.3. Structure of PqsR ligand-binding domain complexed with compounds 6, 12, 18 and 19

Compounds **6**, **12**, **18** and **19** were successfully soaked into a truncated form of PqsR (PqsR$^{94\text{-}309}$) containing the ligand-binding domain of the protein (see S3-6 for additional data including electron density plots and crystallographic table of data collection
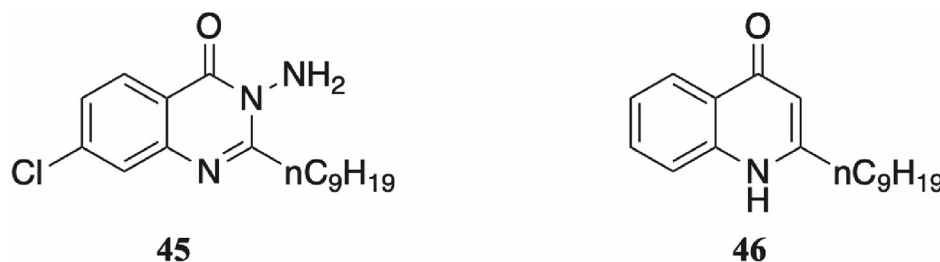
Fig. 4. A previously described PqsR antagonist (**45**) featured a quinazolinone scaffold with a 7-chloro substituted ring. Removal of the chlorine atom led to a 10-fold drop in activity, whilst a 6-chlorine substituted ring was inactive. By contrast, the compound series described in this article found 6-chlorine substitution to be optimal. Both **45** and an endogenous ligand, NHQ (**46**) were successfully crystallised in the PqsR ligand-binding domain [32].

Table 1
In vitro data for all compounds defined as active (inhibits *pqs* system to below 50% at 10 μM). NA denotes inactive compounds which showed a remaining activity above 50% at 10 μM (remaining activity for not active compounds is shown in brackets). Reported values are mean ± SD of *n = 2* replicates. cLogP values were calculated using MarvinSketch based on the algorithm outlined by Viswanadhan et al. [41].

Compound	IC$_{50}$ value in PAO1-L/nM	IC$_{50}$ value in PA14/nM	Predicted cLogP values
6	1046 ± 419	1578 ± 358.0	3.38
8	NA (83%)	NA	2.14
9	NA (52%)	NA	3.03
10	NA (79%)	NA	2.84
11	NA (104%)	NA	2.09
12	397 ± 141.5	650 ± 35.1	3.94
13	1216 ± 44.0	1333 ± 192.5	3.57
14	1563 ± 674.0	1720 ± 882.0	3.73
15	1112 ± 879.5	646 ± 90.2	4.27
16	1572 ± 1119	639 ± 73.5	4.02
17	1360 ± 501.0	683 ± 156.9	4.02
18	313 ± 156.2	342 ± 39.4	4.17
19	298 ± 182.0	265 ± 3.4	4.62
20	1327 ± 189.5	1308 ± 272.0	3.10
21	2048 ± 1241.0	2916 ± 1005.5	3.64
22	244 ± 49.6	123 ± 20.9	4.04
23	NA (89%)	NA	3.98
24	NA (85%)	NA	2.13
25	3545 ± 2934.0	NA	3.50
26	NA (108%)	NA	1.31
27	NA (72%)	NA	4.00
28	NA (83%)	NA	4.02
29	NA (101%)	NA	2.17
30	NA (67%)	NA	3.55
31	NA (85%)	NA	2.18
32	2942 ± 808.0	NA	3.94
33	NA (106%)	NA	4.17
34	NA (95%)	NA	2.93
35	NA (65%)	NA	3.43

and refinement). All four ligands occupied a similar space to that exhibited by a previously described quinazolinone-based inhibitor **45** and two endogenous ligands (HHQ, **3**, and NHQ, **46**) bearing quinolone scaffolds [32,44]. In each case, the quinazolinone core occupies the previously defined B pocket of the LBD [32], and the alkyl chain extends into the open A pocket (Fig. 5). In addition, no major conformational changes occurred to the protein backbone in each of the crystal soaking experiments, as well as the previously reported PqsR crystal structures.

As with **45**, the electron density contours around the halogen atom in each crystal, suggesting that the chlorine has locked the ligand into its defined orientation with the quinazolinone core occupying the B pocket of the PqsR LBD. However, whilst in **45** the carbonyl faces towards the B sub-pocket, the electron density maps suggest that the carbonyl groups of **6**, **12**, **18** and **19** all face towards the opposite face of the LBD in the direction of Thr265. The key result of this is that it enables a hydrogen bond to form between the carbonyl of each of the four compounds with the hydroxyl group of Thr265 (Fig. 6). This is further supported by the observation that the hydroxyl component of Thr265 faces towards the carbonyl in all four structures, in contrast to **45** where it faces towards the chlorine atom and elicits a polar interaction with the halogen.

The importance of this hydrogen bond was further emphasised by the lower activities of compounds **32** and **33**, both featuring a 7-chloro substitution. Repositioning of the chlorine atom removes the possibility of forming a hydrogen bond between the carbonyl and
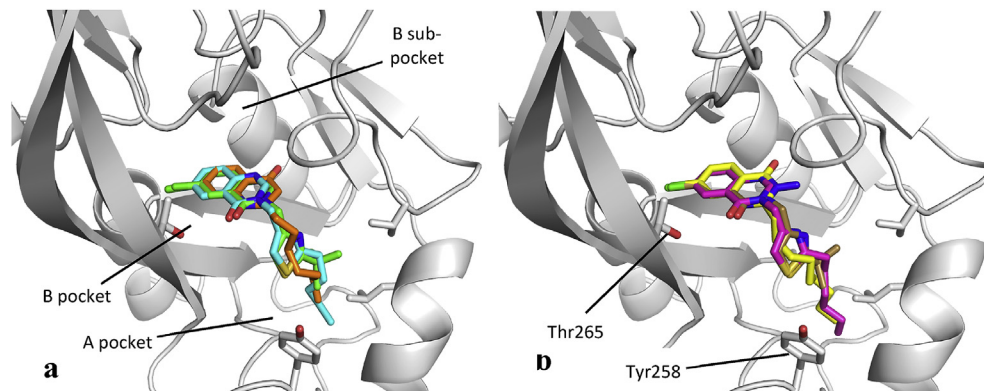
Fig. 5. (a) Overlaying the crystal structures of **12** (green), **18** (cyan) and HHQ (**3**, orange, PDB entry 6Q7U) shows that the core quinazolinone structures occupy almost identical spaces within the LBD, with the alkyl chains extending out to the LBD entrance. Importantly, the carbonyl groups of **12** and **18** face towards Thr265, enabling a H-bond to form, whereas the carbonyl of HHQ faces the opposite wall of the LBD in the direction of the B-sub pocket; (b) The same trends are observed between **6** (gold), **19** (magenta) and **45** (yellow, PDB entry 4JVI). The chlorine atoms of **6**, **19** and **45** directly overlap, demonstrating its importance in locking the structure's conformation NHQ (**46**, PDB entry 4JVD) followed the above trends, but was omitted for clarity. (For interpretation of the references to colour in this figure legend, the reader is referred to the Web version of this article.)
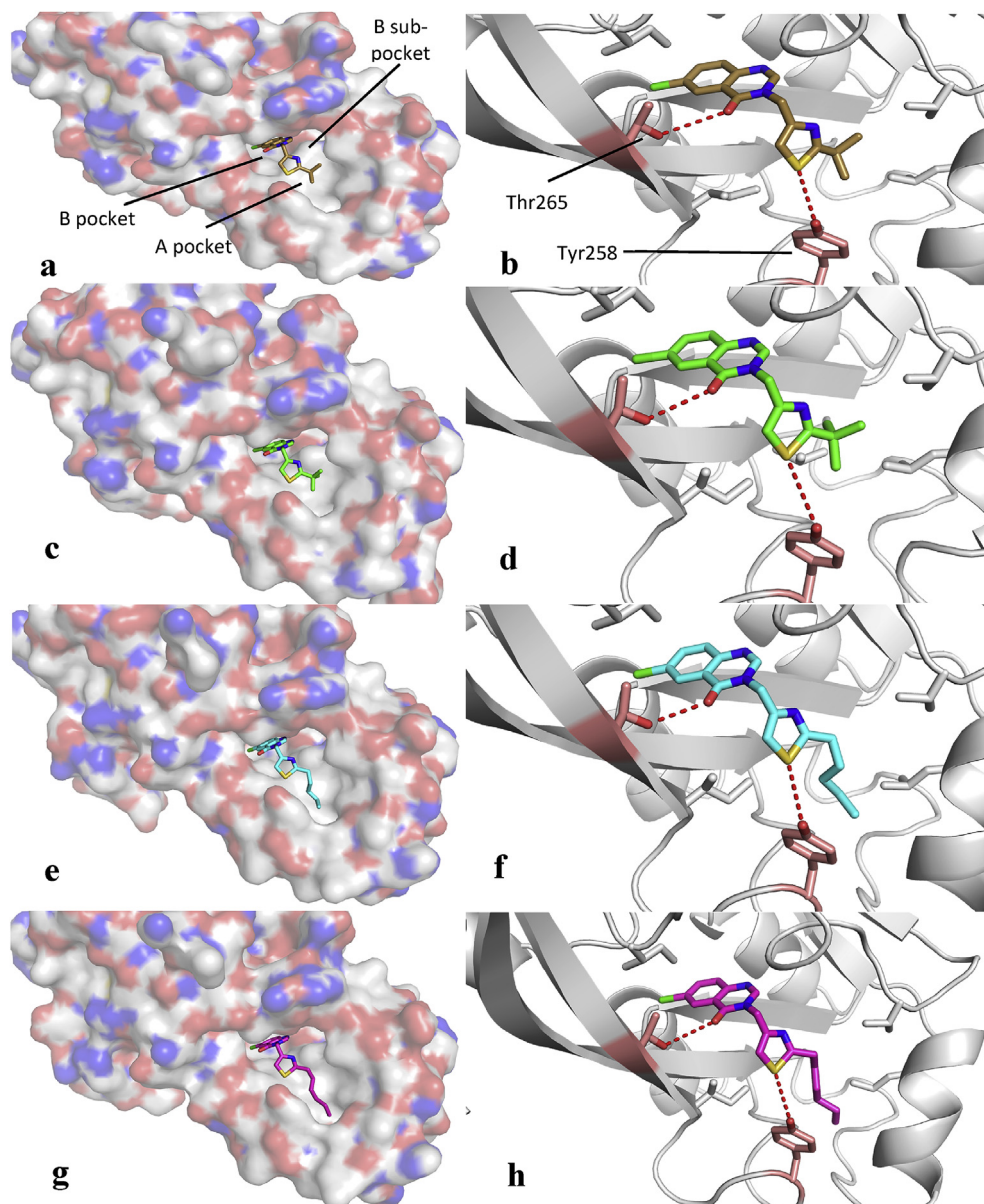
Fig. 6. The binding of **6** into the PqsR LBD as a surface representation (a), and the key binding interactions observed between the carbonyl of **6** and Thr265, and the sulfur atom of **6** and Tyr258 (b). Below these are analogous representations for **12** (c−d), **18** (e−f) and **19** (g−h). In each surface representation the chlorine atom is buried deep into the B pocket, anchoring the ligand in place. Binding modes are seen to be similar in each example, with the hydroxyl of Thr265 turned to face the carbonyl of the quinazolinone, thereby eliciting a H-bond. Furthermore, the sulfur is angled towards the phenol of Tyr258 enabling a polar interaction.

Thr265, hence the significant observed loss of potency.

The thiazole moieties were shown to further contribute to the activity of the series through interactions with Tyr258. In all four crystal structures, the sulfur atom was shown to orient itself facing the tyrosine, likely due to the formation of a polar interaction between the sulfur atom and the phenol group. The inactivity of oxadiazole **7** suggests that the presence of the sulfur aids in binding to the LBD, further implicating the thiazole as an integral component of the series. The role of the sulfur is further highlighted by the inactivity of **35**, whereby the 2,5-thiazole regioisomer is unable to form a polar interaction with Tyr258, leading to a lower potency when compared to the 2,4-thiazole analogue **6**.

The majority of residues in the LBD of PqsR bear aliphatic side chains. As such, hydrophobic interactions are seen to drive activity in both endogenous ligands and synthetic inhibitors. The SAR study indicated that increasing the length and branching of the aliphatic substitution at the 2-position of the thiazole dramatically improved potency. This is observed in the crystal structures, whereby the aliphatic chain forms hydrophobic interactions with the side chains of residues in the A pocket of the LBD. Compounds **6** (IC_{50} = 1.0 μM) and **12** (IC_{50} = 397 nM) are weaker inhibitors than **18** (IC_{50} = 313 nM) and **19** (IC_{50} = 298 nM), as they have shorter alkyl chains unable to form as many hydrophobic interactions with the protein. In particular, **18** and **19** are able to reach Ile186 and Leu189 at the far edge of the A pocket, creating a larger network of hydrophobic interactions and improving the activity over shorter chain analogues such as **6** and **12** (Fig. S4).

2.4. Reduction of pyocyanin production by the PqsR inhibitors

To demonstrate a link between the inhibitory effects of **18** and **19** on PqsR and hence virulence gene expression, pyocyanin production in the PAO1-L was quantified after overnight incubation with either **18** or **19** at a concentration three times higher than their IC$_{50}$, or a vehicle (DMSO) control. Both compounds reduced pyocyanin production to 23% and 36% respectively (Fig. 7), compared with the control. These results indicate that these compounds can attenuate the production of this virulence factor through inhibition of PqsR similar to that shown for other PqsR inhibitors [34,45,46].

2.5. Effect of PqsR inhibitors on cytotoxicity of lung epithelial cells

A cytotoxicity study using A549 lung epithelial cells was conducted with **18** and **19**, to establish the suitability of these compounds for further studies. Compounds **18** and **19** tested at increasing concentrations ranging from 0.1 to 100 μM showed no significant toxicity (Fig. 8). Testing at higher concentrations was not possible as neither compound was fully soluble above this concentration. However, the data showed that both **18** and **19** are not cytotoxic up to 100 μM. Therefore, the therapeutic index is > 292-fold in **18** and > 377-fold in **19** against the A549 cell line relative to the activities calculated for PA14.

3. Conclusion

In summary, a new series of chloro-3-((2-substituted-thiazole)quinazolin-4(3*H*)-one compounds was synthesised and tested in a whole cell bioreporter assay to determine their ability to inhibit PqsR, and subsequently reduce *P. aeruginosa* pyocyanin production. A SAR study showed key contributing functionalities, particularly a long or branched alkyl chain at the 2-position of the thiazole. These studies revealed a preference for chlorine substitution on the 6-position of the quinazolinone ring.

X-ray crystallography into the LBD of PqsR confirmed a binding
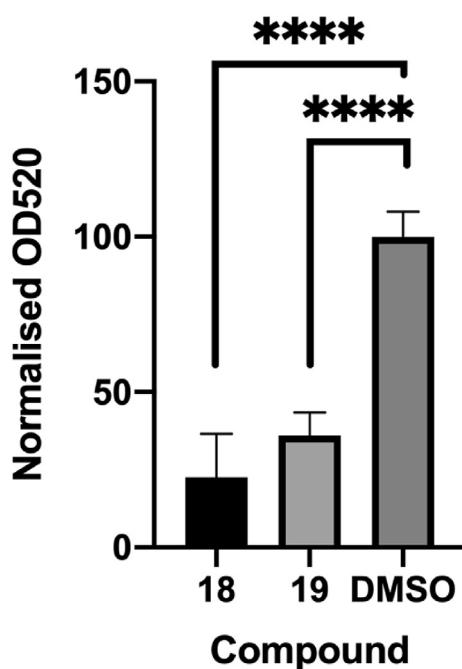
mode similar to that seen in previously described quinazolinone- and quinolone-based inhibitor-bound crystal structures. Further assays confirmed that the most active compounds **18** and **19** were capable of significantly reducing production of the toxin pyocyanin, whilst remaining non-toxic to eukaryotic cells, providing a basis for further pre-clinical studies.

4. Experimental

4.1. Chemistry − general methods

Chemicals and solvents were provided by Fisher Scientific UK, Acros Organics, Sigma-Aldrich, Merck Millipore or Fluorochem. All reactions were monitored by TLC using Merck Silica Gel 60 Å F254 TLC plates or by LC-MS. Unless otherwise stated, all compounds were dried under high vacuum either at rt or within an oven at 40 °C. LC-MS data was collected on a Shimadzu UFLCXR HPLC system coupled to an Applied Biosystems API 2000 LC/MS/MS electrospray ionization (ESI). The column used was a Phenomenex Gemini-NX 3 μm-110Â C18, 50 × 2mm at 40 °C. The flow rate was 0.5 mL/min, the UV detection was at 220 nm and 254 nm. The LC-MS ran for 1 min at 5% B; 5−98% B over 2 min, 98% B for 2 min, 98 to 5% B over 0.5 min and then 5% for 1 min where solvent A: 0.1% formic acid in water; solvent B: acetonitrile. Unless otherwise stated compounds reported had a purity >95%. NMR spectroscopy was performed using a Bruker AV(III) HD 400 NMR spectrometer equipped with a 5 mm BBFO^{+} probe, recording ^{1}H and ^{13}C NMR at 400.25 MHz and 100.66 MHz respectively; or a Bruker AV(III) 500 NMR spectrometer equipped with a 5 mm dual ^{1}H/^{13}C helium-cooled cryoprobe, recording ^{1}H and ^{13}C NMR at 500.13 MHz and 125.77 MHz respectively. NMR data was processed using iNMR (version 5.5.7) referencing spectra to residual solvents. Chemical shifts are quoted as δ: values in ppm; coupling constants J are given in Hz and multiplicities are described as follows: s - singlet, d - doublet, t - triplet, q - quartet, qi - quintet, sep − septet, m − multiplet, app − apparent, br - broad.

4.1.1. General procedure for the preparation of thiazoles 6, 8−23, 32, 33

A solution of the appropriate thioamide or thiourea (0.13 mmol) and α-haloketone **38** or **44** (0.06 mmol) in EtOH (4 mL) was refluxed at 80 °C for 16 h. ^{a} After cooling to room temperature, the reaction mixture was concentrated *in vacuo* and purified through flash column chromatography. Chromatography was run with a gradient of ethyl acetate/petroleum ether (1:2) to pure ethyl acetate. ^{b}

  a Where compound **44** was used as the α-haloketone, 600 μL of acetic acid was added to aid in solubilizing the starting material.
  b Excepting compounds **11** and **26** which were run in DCM/methanol (19:1).

4.1.1.1. 6-Chloro-3-((2-isopropylthiazol-4-yl)methyl)quinazolin-4(3H)-one (**6**).
Obtained **6** (18 mg, 90%) as a white crystal: ^{1}H NMR (DMSO-d_6, 400 MHz) δ 8.54 (s, 1H), 8.05 (d, J = 1.68 Hz, 1H), 7.83 (dd, J = 8.61, 1.72 Hz, 1H), 7.70 (d, J = 8.69 Hz, 1H), 7.39 (s, 1H), 5.25 (s, 2H), 3.24−3.17 (m, 1H), 1.26 (d, J = 6.84 Hz, 6H) ppm; ^{13}C NMR (DMSO-d_6 101 MHz) δ 177.7, 158.9, 150.0, 148.5, 146.6, 134.5, 131.4, 129.5, 125.1, 122.9, 115.7, 45.4, 32.4, 22.8 ppm; LC-MS (+ESI) calculated for $C_{15}H_{14}ClN_3OS$ *m/z* 320.1 (M + H), found *m/z* 320.1 (M + H).

4.1.1.2. 6-Chloro-3-((2-methylthiazol-4-yl)methyl)quinazolin-4(3H)-one (**8**).
Obtained **8** (17 mg, 90%) as an orange crystal: ^{1}H NMR

Fig. 7. Compounds **18** and **19** were shown to significantly reduce pyocyanin production to 23% and 36% respectively against a control of 0.1% DMSO at 3 × the IC$_{50}$ value in *P. aeruginosa* strain PAO1-L.
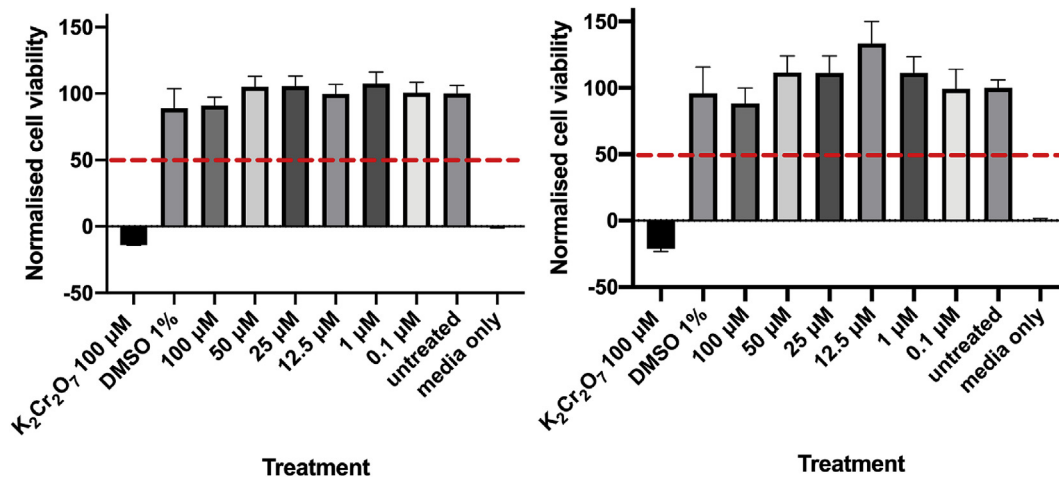
Fig. 8. Cytotoxicity data for (left) **18** and (right) **19** indicated that neither shows significant toxicity up to 100 μM in A549 lung epithelial cells. The lethal dose (LD$_{50}$) value could not be calculated, as cell viability was not reduced to < 50% (indicated by the red dashed line). It was not possible to test at higher compound concentrations due to insolubility in the test buffer. (For interpretation of the references to colour in this figure legend, the reader is referred to the Web version of this article.)

(CDCl$_3$, 400 MHz) δ 8.34 (s, 1H), 8.25 (d, J = 1.24 Hz, 1H), 7.69−7.63 (m, 2H), 7.20 (s, 1H), 5.22 (s, 2H), 2.66 (s, 3H) ppm; ^{13}C NMR (CDCl$_3$ 101 MHz) δ 159.9, 149.4, 146.9, 146.6, 134.7, 133.1, 129.2, 126.2, 123.2, 117.7, 45.4, 29.7, 19.1 ppm; LC-MS (+ESI) calculated for C$_{13}$H$_{10}$ClN$_3$OS m/z 292.0 (M + H), found m/z 292.1 (M + H).

4.1.1.3. 6-Chloro-3-((2-(trifluoromethyl)thiazol-4-yl)methyl)quinazolin-4(3H)-one (9). Obtained **9** (3.5 mg, 16%) as a yellow solid: ^{1}H NMR (CDCl$_3$, 400 MHz) δ 8.35 (s, 1H), 8.24 (d, J = 1.64 Hz, 1H), 7.71 (s, 1H), 7.69−7.66 (m, 2H), 5.32 (s, 2H) ppm; LC-MS (+ESI) calculated for C$_{13}$H$_7$ClF$_3$N$_3$OS m/z 346.0 (M + H), found m/z 346.1 (M + H).

4.1.1.4. 6-Chloro-3-((2-ethylthiazol-4-yl)methyl)quinazolin-4(3H)-one (10). Obtained **10** (14 mg, 70%) as a white solid: ^{1}H NMR (CDCl$_3$, 400 MHz) δ 8.28 (s, 1H), 8.15 (s, 1H), 7.61−7.55 (m, 2H), 7.14 (s, 1H), 5.16 (s 2H), 2.90 (q, J = 7.52 Hz, 2H), 1.27 (t, J = 7.56 Hz, 3H) ppm; ^{13}C NMR (CDCl$_3$ 101 MHz) δ 173.9, 159.7, 149.1, 147.0, 146.5, 134.6, 132.9, 129.1, 126.0, 123.1, 117.1, 45.3, 26.8, 14.0 ppm; LC-MS (+ESI) calculated for C$_{14}$H$_{12}$ClN$_3$OS m/z 306.0 (M + H), found m/z 306.1 (M + H).

4.1.1.5. 2-(4-((6-Chloro-4-oxoquinazolin-3(4H)-yl)methyl)thiazol-2-yl)acetonitrile (11). Obtained **11** (18 mg, 90%) as a red-orange solid: ^{1}H NMR (CDCl$_3$, 400 MHz) δ 8.32 (s, 1H), 8.23 (d, J = 1.80 Hz, 1H), 7.70−7.64 (m, 2H), 7.43 (s, 1H), 5.24 (s, 2H), 4.06 (s, 2H) ppm; ^{13}C NMR (CDCl$_3$ 101 MHz) δ 159.8, 158.4, 150.6, 146.6, 146.5, 134.8, 133.3, 129.2, 126.1, 123.1, 119.8, 115.0, 45.3, 22.2 ppm; LC-MS (+ESI) calculated for C$_{14}$H$_9$ClN$_4$OS m/z 317.0 (M + H), found m/z 317.2 (M + H).

4.1.1.6. 3-((2-(Tert-butyl)thiazol-4-yl)methyl)-6-chloroquinazolin-4(3H)-one (12). Obtained **12** (9.0 mg, 43%) as a white crystal: ^{1}H NMR (CDCl$_3$, 400 MHz) δ 8.43 (s, 1H), 8.27 (d, J = 1.80 Hz, 1H), 7.70−7.65 (m, 2H), 7.19 (s, 1H), 5.26 (s, 2H), 1.40 (s, 9H) ppm; ^{13}C NMR (CDCl$_3$ 101 MHz) δ182.4, 159.9, 148.9, 147.1, 146.6, 134.7, 133.1, 129.2, 126.2, 123.2, 116.7, 45.3, 37.8, 30.9 ppm; LC-MS (+ESI) calculated for C$_{16}$H$_{16}$ClN$_3$OS m/z 334.1 (M + H), found m/z 334.2 (M + H).

4.1.1.7. 6-Chloro-3-((2-isobutylthiazol-4-yl)methyl)quinazolin-4(3H)-one (13). Obtained **13** (11 mg, 53%) as a silver crystal: ^{1}H NMR (DMSO-d$_6$, 400 MHz) δ 8.54 (s, 1H), 8.07 (d, J = 2.36 Hz, 1H),

7.86 (dd, J = 8.69, 2.40 Hz, 1H), 7.72 (d, J = 8.69 Hz, 1H), 7.42 (s, 1H), 5.25 (s, 2H), 2.77 (d, J = 7.08 Hz, 2H), 1.95 (qt, J = 6.72, 6.72 Hz, 1H), 0.88 (d, J = 6.65 Hz, 6H) ppm; ^{13}C NMR (DMSO-d$_6$, 101 MHz) δ 170.1, 158.9, 150.1, 148.6, 146.6, 134.5, 131.4, 129.5, 125.1, 122.9, 116.4, 45.3, 41.2, 29.1, 21.9 ppm; LC-MS (+ESI) calculated for C$_{16}$H$_{16}$ClN$_3$OS m/z 334.1 (M + H), found m/z 334.1 (M + H).

4.1.1.8. 3-((2-Butylthiazol-4-yl)methyl)-6-chloroquinazolin-4(3H)-one (14). Obtained **14** (29 mg, 88%) as a yellow crystal: ^{1}H NMR (400 MHz, CDCl$_3$) δ 8.34 (s, 1H), 8.23 (dd, J = 2.00, 0.87 Hz, 1H), 7.67−7.60 (m, 2H), 7.19 (s, 1H), 5.22 (s, 2H), 2.92 (t, J = 7.74 Hz 2H), 1.71 (tt, J = 7.70, 7.70 Hz, 2H), 1.38 (tq, J = 7.45, 7.45 Hz, 3H), 0.90 (t, J = 7.38 Hz, 5H) ppm; ^{13}C NMR (101 MHz, DMSO) δ 171.4, 158.9, 150.0, 148.6, 146.7, 134.5, 131.4, 129.6, 125.1, 122.9, 116.2, 45.4, 32.2, 31.4, 21.5, 13.5 ppm; LC-MS (+ESI) calculated for C$_{16}$H$_{16}$ClN$_3$OS m/z 334.1 (M + H), found m/z 334.1 (M + H).

4.1.1.9. 6-Chloro-3-((2-(pentan-2-yl)thiazol-4-yl)methyl)quinazolin-4(3H)-one (15). Obtained **15** (11 mg, 45%) as a yellow oily solid: ^{1}H NMR (CDCl$_3$, 400 MHz) δ 8.37 (s, 1H), 8.25 (d, J = 1.52 Hz, 1H), 7.69−7.63 (m, 2H), 7.20 (s, 1H), 5.24 (s, 2H), 3.14 (qt, J = 6.96, 6.96 Hz, 1H), 1.77−1.53 (m, 2H), 1.33−1.25 (m, 5H), 0.88 (t, J = 7.32 Hz, 3H) ppm; ^{13}C NMR (CDCl$_3$ 101 MHz) δ 178.6, 159.8, 148.8, 147.0, 146.5, 134.7, 133.1, 129.1, 126.2, 123.2, 116.7, 45.3, 39.9, 38.3, 21.4, 20.3, 13.9 ppm; LC-MS (+ESI) calculated for C$_{17}$H$_{18}$ClN$_3$OS m/z 348.1 (M + H), found m/z 348.2 (M + H).

4.1.1.10. 6-Chloro-3-((2-(2-methylbutyl)thiazol-4-yl)methyl)quinazolin-4(3H)-one (16). Obtained **16** (20 mg, 91%) as a colourless oil: ^{1}H NMR (CDCl$_3$, 400 MHz) δ 8.35 (s, 1H), 8.25 (d, J = 1.64 Hz, 1H), 7.69−7.63 (m, 2H), 7.21 (s, 1H), 5.24 (s, 2H), 2.94 (dd, J = 14.61, 6.08 Hz, 1H), 2.75 (dd, J = 14.61, 8.09 Hz, 1H), 1.89−1.80 (m, 1H), 1.46−1.14 (m, 2H), 0.92−0.87 (m, 6H) ppm; ^{13}C NMR (CDCl$_3$ 101 MHz) δ 171.6, 159.7, 149.2, 146.9, 146.6, 134.7, 129.2, 126.2, 123.0, 117.3, 45.4, 40.3, 36.0, 29.7, 29.1, 19.0, 11.3 ppm; LC-MS (+ESI) calculated for C$_{17}$H$_{18}$ClN$_3$OS m/z 348.1 (M + H), found m/z 348.2 (M + H).

4.1.1.11. 6-Chloro-3-((2-isopentylthiazol-4-yl)methyl)quinazolin-4(3H)-one (17). Obtained **17** (13 mg, 71%) as a white crystal: ^{1}H NMR (CDCl$_3$, 400 MHz) δ 8.36 (s, 1H), 8.25 (d, J = 1.48 Hz, 1H), 7.69−7.63 (m, 2H), 7.20 (s, 1H), 5.23 (s, 2H), 2.95 (t, J = 7.61 Hz, 2H),

1.65–1.62 (m, 3H), 0.93 (d, $J = 6.04$ Hz, 6H); ^{13}C NMR (CDCl$_3$ 101 MHz) δ 172.9, 159.8, 149.2, 146.9, 134.7, 133.0, 129.2, 126.2, 123.3, 117.2, 45.4, 38.9, 31.5, 29.7, 27.7, 23.3 ppm; LC-MS (+ESI) calculated for C$_{17}$H$_{18}$ClN$_3$OS m/z 348.1 (M + H), found m/z 348.2 (M + H).

4.1.1.12. 6-Chloro-3-((2-pentylthiazol-4-yl)methyl)quinazolin-4(3H)-one (18). Obtained **18** (20 mg, 90%) as a white crystal: ^{1}H NMR (CDCl$_3$, 400 MHz) δ 8.35 (s, 1H), 8.26 (d, $J = 1.92$ Hz, 1H), 7.69–7.63 (m, 2H), 7.20 (s, 1H), 5.23 (s, 2H), 2.93 (t, $J = 7.68$ Hz, 2H), 1.77–1.69 (m, 2H), 1.37–1.33 (m, 4H), 0.90 (t, $J = 6.93$ Hz, 3H) ppm; ^{13}C NMR (CDCl$_3$ 101 MHz) δ 172.8, 159.9, 149.1, 147.0, 146.6, 134.7, 133.1, 129.2, 126.2, 123.2, 117.2, 45.4, 33.4, 31.3, 29.6, 22.3, 13.9 ppm; LC-MS (+ESI) calculated for C$_{17}$H$_{18}$ClN$_3$OS m/z 348.1 (M + H), found m/z 348.2 (M + H).

4.1.1.13. 6-Chloro-3-((2-hexylthiazol-4-yl)methyl)quinazolin-4(3H)-one (19). Obtained **19** (15 mg, 66%) as a white crystal: ^{1}H NMR (CDCl$_3$, 400 MHz) δ 8.36 (s, 1H), 8.25 (d, $J = 1.72$ Hz, 1H), 7.69–7.64 (m, 2H), 7.21 (s, 1H), 5.23 (s, 2H), 2.94 (t, $J = 7.89$ Hz, 2H), 1.74 (tt, $J = 7.64, 7.64$ Hz, 2H), 1.40–1.33 (m, 4H), 1.30–1.27 (m, 4H), 0.86 (t, $J = 6.93$ Hz, 3H) ppm; ^{13}C NMR (CDCl$_3$ 101 MHz) δ 172.8, 159.8, 149.1, 146.9, 146.5, 134.7, 133.1, 129.1, 126.1, 123.2, 117.2, 45.4, 33.4, 31.4, 29.9, 28.7, 22.4, 14.0 ppm; LC-MS (+ESI) calculated for C$_{18}$H$_{20}$ClN$_3$OS m/z 362.1 (M + H), found m/z 362.3 (M + H).

4.1.1.14. 6-Chloro-3-((2-(furan-2-yl)thiazol-4-yl)methyl)quinazolin-4(3H)-one (20). Obtained **20** (17 mg, 80%) as a white crystal: ^{1}H NMR (CDCl$_3$, 400 MHz) δ 8.40 (s, 1H), 8.26 (d, $J = 1.88$ Hz, 1H), 7.67 (d, $J = 2.20$ Hz, 1H), 7.66 (s, 1H), 7.50 (d, $J = 1.09$ Hz, 1H), 7.32 (s, 1H), 6.97 (d, $J = 3.64$ Hz, 1H), 6.52 (dd, $J = 3.36, 1.80$ Hz, 1H), 5.29 (s, 2H) ppm; ^{13}C NMR (CDCl$_3$ 101 MHz) δ 159.9, 158.9, 150.6, 148.5, 146.9, 146.6, 143.9, 134.8, 133.2, 129.2, 126.2, 123.2, 117.3, 112.3, 109.5, 45.4 ppm; LC-MS (+ESI) calculated for C$_{16}$H$_{10}$ClN$_3$O$_2$S m/z 344.0 (M + H), found m/z 344.1 (M + H).

4.1.1.15. 6-Chloro-3-((2-(2-(furan-2-yl)vinyl)thiazol-4-yl)methyl) quinazolin-4(3H)-one (21). Obtained **21** (12 mg, 51%) as a cream solid. A minor impurity remained, giving a final purity of 91.7% as determined by ^{1}H NMR: ^{1}H NMR (DMSO-d_6, 400 MHz) δ 8.60 (s, 1H), 8.09 (d, $J = 2.32$ Hz, 1H), 7.88 (dd, $J = 8.73, 2.36$ Hz, 1H), 7.77–7.73 (m, 2H), 7.54 (s, 1H), 7.29 (d, $J = 16.09$ Hz, 1H), 7.08 (d, $J = 16.09$ Hz, 1H), 6.79 (d, $J = 3.24$ Hz, 1H), 6.59 (dd, $J = 2.88, 1.64$ Hz, 1H), 5.30 (s, 2H) ppm; ^{13}C NMR (101 MHz, DMSO) δ 166.0, 159.0, 151.7, 151.1, 148.6, 146.7, 144.5, 134.6, 131.5, 129.6, 125.1, 122.9, 121.5, 118.3, 117.0, 112.7, 112.5, 45.5 ppm; LC-MS (+ESI) calculated for C$_{18}$H$_{12}$ClN$_3$O$_2$S m/z 370.0 (M + H), found m/z 370.2 (M + H).

4.1.1.16. 6-Chloro-3-((2-phenylthiazol-4-yl)methyl)quinazolin-4(3H)-one (22). Obtained **22** (20 mg, 92%) as a white solid: ^{1}H NMR (CDCl$_3$, 400 MHz) δ 8.47 (s, 1H), 8.27 (d, $J = 1.72$ Hz, 1H), 7.92–7.89 (m, 2H), 7.70–7.64 (m, 2H), 7.43–7.41 (m, 3H), 7.36 (s, 1H), 5.32 (s, 2H) ppm; ^{13}C NMR (CDCl$_3$ 101 MHz) δ 169.1, 159.9, 150.7, 147.1, 146.6, 134.7, 133.1, 133.1, 130.4, 129.2, 129.0, 126.5, 126.2, 123.2, 117.9, 45.5 ppm; LC-MS (+ESI) calculated for C$_{18}$H$_{12}$ClN$_3$OS m/z 354.0 (M + H), found m/z 354.2 (M + H).

4.1.1.17. 6-Chloro-3-((2-(4-nitrophenyl)thiazol-4-yl)methyl)quinazolin-4(3H)-one (23). Obtained **23** (15 mg, 48%) as a white crystal: ^{1}H NMR (400 MHz, DMSO-d_6) δ 8.66 (s, 1H), 8.36–8.28 (m, 2H), 8.15 (d, $J = 2.08$ Hz, 1H), 8.14–8.06 (m, 2H), 7.91–7.83 (m, 2H), 7.75 (d, $J = 8.74$ Hz, 1H), 5.39 (s, 2H) ppm; LC-MS (+ESI) calculated for C$_{18}$H$_{11}$ClN$_4$O$_3$S m/z 399.0 (M + H), found m/z 399.1 (M + H).

4.1.1.18. 6-Chloro-3-((2-((2-methoxyethyl)amino)thiazol-4-yl) methyl)quinazolin-4(3H)-one (24). Obtained **24** (34 mg, 51%) as a cream solid: ^{1}H NMR (DMSO-d_6, 400 MHz) δ 8.47 (s, 1H), 8.08 (d, $J = 2.67$ Hz, 1H), 7.85 (dd, $J = 9.06, 2.70$ Hz, 1H), 7.72–7.67 (m, 2H), 6.42 (s, 1H), 5.00 (s, 2H), 3.41 (t, $J = 5.39$ Hz, 2H), 3.32 (t, $J = 4.91$ Hz, 2H), 3.21 (s, 3H) ppm; ^{13}C NMR (DMSO-d_6, 101 MHz) δ 169.1, 158.9, 148.6, 146.6, 146.3, 134.5, 131.3, 129.5, 125.1, 122.9, 102.8, 70.1, 57.9, 45.5, 43.9 ppm; LC-MS (+ESI) calculated for C$_{15}$H$_{15}$ClN$_4$O$_2$S m/z 351.1 (M + H), found m/z 350.6 (M + H).

4.1.1.19. 3-((2-(Butylamino)thiazol-4-yl)methyl)-6-chloroquinazolin-4(3H)-one (25). Obtained **25** (16 mg, 24%) as a white crystal: ^{1}H NMR (DMSO-d_6, 400 MHz) δ 8.46 (s, 1H), 8.08 (d, $J = 2.65$ Hz, 1H), 7.86 (s, dd, $J = 8.68, 2.65$ Hz, 1H), 7.72 (d, $J = 8.68$ Hz, 1H), 7.61 (t, $J = 5.67$ Hz, 1H), 6.42 (s, 1H), 5.00 (s, 2H), 3.11 (dt, $J = 6.87, 5.20$ Hz, 2H), 1.46 (tt, $J_1 = J_2 = 7.07$ Hz), 1.28 (tq, $J = 7.33, 7.33$ Hz, 2H), 0.83 (t, $J = 7.32$ Hz, 3H) ppm; ^{13}C NMR (DMSO-d_6, 101 MHz) δ 169.4, 158.9, 148.6, 146.7, 146.5, 134.5, 131.3, 129.5, 125.1, 122.9, 102.4, 45.5, 44.2, 30.7, 19.5, 13.6 ppm; LC-MS (+ESI) calculated for C$_{16}$H$_{17}$ClN$_4$OS m/z 349.1 (M + H), found m/z 348.9 (M + H).

4.1.1.20. 2-(4-((6-Chloro-4-oxoquinazolin-3(4H)-yl)methyl)thiazol-2-yl)guanidine (26). Obtained **26** (13 mg, 62%) as a cream solid: ^{1}H NMR (DMSO-d_6, 400 MHz) δ 8.55 (s, 1H), 8.08 (d, $J = 2.40$ Hz, 1H), 7.85–7.83 (m, 1H), 7.70 (dd, $J = 8.77, 2.36$ Hz, 1H), 7.04 (br s, 4H), 5.06 (s, 2H) ppm; LC-MS (+ESI) calculated for C$_{13}$H$_{11}$ClN$_6$OS m/z 335.0 (M + H), found m/z 335.2 (M + H).

4.1.2. General procedure for the preparation of 3-((2-amino) thiazol-5-yl)methyl)quinazolin-4(3H)-one compounds 27–31 from 34

A solution of **34** (0.32 mmol) and appropriate amine (0.96 mmol) in DMSO (0.5 mL) was refluxed at 100–130 °C (dependent on the boiling point of the amine) for 16 h. The reaction mixture was cooled to room temperature, diluted with water and extracted with ethyl acetate (3 × 20 mL). The combined organic layers were dried over brine and concentrated *in vacuo*. Purification through flash column chromatography in ethyl acetate/petroleum ether (4:1) to ethyl acetate to methanol/ethyl acetate (19:1) yielded products **27–31** in yields of 21–84%.

4.1.2.1. 6-Chloro-3-((2-(4-methylpiperidin-1-yl)thiazol-5-yl)methyl) quinazolin-4-(3H)-one (27). Obtained **27** (86 mg, 72%) as a yellow solid: ^{1}H NMR (DMSO-d_6, 400 MHz) δ 8.57 (s, 1H), 8.12 (d, $J = 2.28$ Hz, 1H), 7.88 (dd, $J = 8.82, 2.67$ Hz, 1H), 7.72 (d, $J = 8.70$ Hz, 1H), 7.26 (s, 1H), 5.20 (s, 2H), 3.80–3.77 (m, 2H), 2.92 (ddd, $J = 3.02, 3.02, 12.44$ Hz, 2H), 1.65–1.61 (m, 2H), 1.58–1.51 (m, 1H), 1.10 (dddd, $J = 4.14, 4.14, 4.14, 11.93$ Hz, 2H), 0.89 (d, $J = 6.16$ Hz, 3H) ppm; ^{13}C NMR (DMSO-d_6, 101 MHz) δ 171.7, 159.0, 147.8, 146.6, 140.2, 134.6, 131.6, 129.6, 125.0, 122.6, 119.8, 48.2, 42.2, 32.7, 30.0, 21.5 ppm; LC-MS (+ESI) calculated for C$_{18}$H$_{19}$ClN$_4$OS m/z 375.1 (M + H), found m/z 374.6 (M + H).

4.1.2.2. 6-Chloro-3-((2-(cyclohexylamino)thiazol-5-yl)methyl)quinazolin-4-(3H)-one (28). Obtained **28** (25 mg, 21%) as a brown solid: ^{1}H NMR (DMSO-d_6, 400 MHz) δ 8.55 (s, 1H), 8.11 (d, $J = 2.52$ Hz, 1H), 8.67 (dd, $J = 8.55, 2.21$ Hz, 1H), 7.72 (d, $J = 8.78$ Hz, 1H), 7.50 (d, $J = 7.48$ Hz, 1H), 7.11 (s, 1H), 5.15 (s, 2H), 3.39–3.34 (m, 1H), 1.89–1.84 (m, 2H), 1.69–1.64 (m, 3H), 1.56–1.51 (m, 1H), 1.31–1.11 (m, 4H) ppm; ^{13}C NMR (DMSO-d_6, 101 MHz) δ 169.0, 159.0, 147.9, 146.6, 139.5, 134.6, 131.6, 129.6, 125.0, 122.7, 117.9, 53.0, 42.3, 32.3, 25.3, 24.4 ppm; LC-MS (+ESI) calculated for C$_{18}$H$_{19}$ClN$_4$OS m/z 375.1 (M + H), found m/z 374.6 (M + H).

4.1.2.3. 6-Chloro-3-((2-(2-hydroxyethyl(methyl)amino)thiazol-5-yl) methyl)quinazolin-4-(3H)-one (29). Obtained **29** (94 mg, 84%) as a yellow solid: ^{1}H NMR (DMSO-d_6, 400 MHz) δ 8.57 (s, 1H), 8.12 (d, $J = 2.52$ Hz, 1H), 7.88 (dd, $J = 8.3$, 2.51 Hz, 1H), 7.72 (d, $J = 8.8$ Hz, 1H), 7.24 (s, 1H), 5.20 (s, 2H), 4.75 (t, $J = 5.74$, 1H), 3.55 (dt, $J = 6.31$, 6.31 Hz, 2H), 3.43 (t, $J = 5.75$, 2H), 2.99 (s, 3H) ppm; ^{13}C NMR (DMSO-d_6, 101 MHz) δ 171.1, 159.0, 147.8, 146.6, 140.3, 134.6, 131.6, 129.5, 125.0, 122.6, 119.0, 58.1, 54.7, 42.3, 40.4 ppm; LC-MS (+ESI) calculated for $C_{15}H_{15}ClN_4O_2S$ *m/z* 351.1 (M + H), found *m/z* 350.6 (M + H).

4.1.2.4. 3-((2-(Butylamino)thiazol-5-yl)methyl)-6-chloroquinazolin-4(3H)-one (30). Obtained **30** (46 mg, 41%) as a yellow solid: ^{1}H NMR (DMSO-d_6, 400 MHz) δ 8.54 (s, 1H), 8.11 (d, $J = 2.22$ Hz, 1H), 7.85 (dd, $J = 8.03$, 2.22 Hz, 1H), 7.70 (d, $J = 7.75$ Hz, 1H), 7.56 (t, $J = 5.54$ Hz, 1H), 7.13 (s, 1H), 5.15 (s, 2H), 3.13 (dt, $J = 6.96$, 6.96 Hz, 2H), 1.46 (tt, $J = 7.01$, 7.01 Hz, 2H), 1.29 (tq, $J = 7.36$, 7.36 Hz, 2H), 0.85 (t, $J = 7.41$ Hz, 3H) ppm; ^{13}C NMR (CDCl$_3$, 101 MHz) δ 172.0, 160.1, 146.7, 145.9, 139.8, 135.0, 133.5, 129.4, 126.3, 123.2, 118.8, 46.0, 43.2, 31.4, 20.1, 13.8 ppm; LC-MS (+ESI) calculated for $C_{16}H_{17}ClN_4OS$ *m/z* 349.1 (M + H), found *m/z* 348.7 (M + H).

4.1.2.5. 6-Chloro-3-((2-((2-methoxyethyl)amino)thiazol-5-yl) methyl)quinazolin-4-(3H)-one (31). Obtained **31** (24 mg, 22%) as a yellow solid: ^{1}H NMR (DMSO-d_6, 400 MHz) δ 8.55 (s, 1H), 8.11 (d, $J = 2.04$ Hz, 1H), 8.08 (s, br, 1H), 7.86 (dd, $J = 8.85$, 2.85 Hz, 1H), 7.71 (d, $J = 8.85$ Hz, 1H), 7.21 (s, 1H), 5.16 (s, 2H), 3.43 (t, $J = 5.37$ Hz, 2H), 3.38−3.34 (m, 2H), 3.23 (s, 3H) ppm; ^{13}C NMR (CDCl$_3$, 101 MHz) δ 171.7, 160.2, 146.9, 145.7, 136.6, 135.1, 133.6, 129.4, 126.3, 123.0, 118.0, 70.5, 59.0, 45.9, 43.2 ppm; LC-MS (+ESI) calculated for $C_{15}H_{15}ClN_4O_2S$ *m/z* 351.1 (M + H), found *m/z* 350.7 (M + H).

4.1.2.6. 3-((2-Tert-butyl)thiazol-4-yl)methyl)-7-chloroquinazolin-4(3H)-one (32). Obtained **32** (2.0 mg, 11%) as a white solid: ^{1}H NMR (400 MHz, CDCl$_3$) δ 8.47 (s, 1H), 8.25 (d, $J = 8.56$ Hz, 1H), 7.74 (d, $J = 1.99$ Hz, 1H), 7.47 (dd, $J = 8.55$, 2.01 Hz, 1H), 7.22 (s, 1H), 5.28 (s, 2H), 1.43 (s, 9H) ppm; ^{13}C NMR (126 MHz, CDCl$_3$) δ 182.9, 160.3, 148.7, 148.7, 148.3, 140.8, 128.4, 128.1, 127.0, 120.6, 117.1, 45.2, 38.0, 31.0 ppm; LC-MS (+ESI) calculated for $C_{16}H_{16}ClN_3OS$ *m/z* 334.1 (M + H), found *m/z* 334.2 (M + H).

4.1.2.7. 7-Chloro-3-((2-pentylthiazol-4-yl)methyl)quinazolin-4(3H)-one (33). Obtained **33** (2.0 mg, 11%) as a white solid: ^{1}H NMR (400 MHz, CDCl$_3$) δ 8.20 (d, $J = 8.57$ Hz, 1H), 7.99 (s, 1H), 7.76 (d, $J = 2.00$ Hz, 1H), 7.47 (dd, $J = 8.57$, 2.00 Hz, 1H), 4.98 (s, 1H), 3.83 (s, 2H), 2.64 (t, $J = 7.55$ Hz, 2H), 1.73−1.67 (m 2H), 1.36−1.28 (m, 4H), 0.94−0.86 (m, 3H) ppm; ^{13}C NMR (126 MHz, CDCl$_3$) δ 199.0, 197.2, 160.1, 148.3, 147.9, 141.3, 128.5, 128.5, 126.9, 120.2, 53.8, 43.6, 36.5, 31.2, 25.3, 22.4, 14.0 ppm; LC-MS (+ESI) calculated for $C_{17}H_{18}ClN_3OS$ *m/z* 348.1 (M + H), found *m/z* 348.0 (M + H).

4.1.2.8. 6-Chloro-3-((2-chlorothiazol-5-yl)methyl)quinazolin-4(3H)-one (34). A solution of **36** (1.00 g, 5.50 mmol) in toluene (15 mL) was treated with KOH (620 mg, 11.10 mmol) and TBAI (193 mg, 0.55 mmol) and heated at 70 °C for 10 min. To this was added 2-chloro-5-(chloromethyl)thiazole (740 μL, 6.60 mmol) dropwise and stirred for 1 h at 70 °C forming a dark brown solution. The reaction mixture was cooled to room temperature, diluted with water and extracted with ethyl acetate (4 × 20 mL). The combined organic layers were dried over Na$_2$SO$_4$ and filtered. The organic layer was concentrated *in vacuo* and triturated with diethyl ether (3 × 20 mL), yielding **34** (1.53 g, 89%) as a yellow solid: ^{1}H NMR (DMSO-d_6, 400 MHz) δ 8.62 (s, 1H), 8.13 (d, $J = 2.57$ Hz, 1H), 7.89 (dd, $J = 8.89$, 2.57 Hz, 1H), 7.81 (s, 1H), 7.73 (d, $J = 8.61$ Hz, 1H), 5.36 (s, 2H) ppm; ^{13}C NMR (CDCl$_3$, 101 MHz) δ 160.1, 154.2, 146.6, 145.3,

141.3, 135.4, 134.2, 134.0, 129.6, 126.3, 123.0, 43.1 ppm; LC-MS (+ESI) calculated for $C_{12}H_7Cl_2N_3OS$ *m/z* 312.0 (M + H), found *m/z* 311.8 (M + H).

4.1.2.9. 6-Chloro-3-((2-isopropylthiazol-5-yl)methyl)quinazolin-4(3H)-one (35). To a solution of intermediate **41** (140 mg, 0.58 mmol) in acetonitrile (5 mL) was added acetic acid (500 μL) and **40** (55 mg, 0.29 mmol) and stirred at 100 °C for 2 h. The reaction mixture was cooled to room temperature, neutralised with saturated NaHCO$_3$, and extracted with ethyl acetate (3 × 10 mL). The combined organic layers were dried over brine, concentrated *in vacuo* and purified through HPLC, yielding **35** (2 mg, 2%) as a white solid: ^{1}H NMR (400 MHz, DMSO-d_6) δ 8.63 (s, 1H), 8.12 (d, $J = 2.51$ Hz, 1H), 7.88 (dd, $J = 8.71$, 2.53 Hz, 1H), 7.77 (s, 1H), 7.72 (d, $J = 8.69$ Hz, 1H), 5.37 (s, 2H), 3.20 (sept, $J = 6.87$ Hz, 1H), 1.27 (d, $J = 6.85$ Hz, 6H) ppm; ^{13}C NMR (126 MHz, DMSO) δ 178.2, 165.8, 147.9, 146.6, 142.2, 134.8, 131.7, 131.6, 129.7, 125.1, 122.7, 41.8, 32.6, 22.7 ppm; LC-MS (+ESI) calculated for $C_{15}H_{14}ClN_3OS$ *m/z* 320.1 (M + H), found *m/z* 320.2 (M + H).

4.1.2.10. 6-Chloroquinazolin-4(3H)-one (36). A solution of 2-amino-5-chlorobenzoic acid (4.99 g, 29.00 mmol) and formamide (20 mL) was refluxed at 150 °C for 16 h, forming a brown precipitate. The reaction mixture was cooled to room temperature and 20 g ice was added. The mixture was left to stand for 1 h, then the precipitate filtered and concentrated *in vacuo*, yielding **36** (5.13 g, 97%) as brown microcrystals: ^{1}H NMR (DMSO-d_6, 400 MHz) δ 12.44 (br s, 1H), 8.12 (s, 1H), 8.06 (d, $J = 2.40$ Hz, 1H), 7.85 (dd, $J = 8.65$, 2.52 Hz, 1H), 7.70 (d, $J = 8.77$ Hz, 1H) ppm; ^{13}C NMR (DMSO-d_6, 101 MHz) δ 160.3, 152.6, 146.5, 134.9, 131.5, 130.0, 125.3, 124.4 ppm; LC-MS (+ESI) calculated for $C_8H_5ClN_2O$ *m/z* 181.0 (M + H), found *m/z* 181.2 (M + H).

4.1.2.11. 6-Chloro-3-(2-oxopropyl)quinazolin-4(3H)-one (37). To a solution of **36** (1.60 g, 6.76 mmol) in anhydrous NMP was added NaH (650 mg, 27.08 mmol) in small portions, forming a white precipitate. After stirring for 30 min the solution returned to a clear brown state and chloroacetone (2.4 mL, 29.28 mmol) was added dropwise forming a deep red solution. The solution was concentrated *in vacuo* and recrystallised in 3:1 hexane/ethyl acetate, yielding **37** (1.80 g, 86%) as white needle crystals: ^{1}H NMR (DMSO-d_6, 400 MHz) δ 8.25 (s, 1H), 8.07 (d, $J = 2.40$ Hz, 1H), 7.89 (dd, $J = 8.73$, 2.48 Hz, 1H), 7.74 (d, $J = 8.73$ Hz, 1H), 4.98 (s, 2H), 2.25 (s, 3H) ppm; ^{13}C NMR (CDCl$_3$, 101 MHz) δ 199.7, 159.87, 146.7, 146.4, 135.0, 133.3, 129.3, 126.1, 122.9, 54.7, 27.5 ppm; LC-MS (+ESI) calculated for $C_{11}H_9ClN_2O_2$ *m/z* 237.0 (M + H), found *m/z* 237.1 (M + H).

4.1.2.12. 3-(3-Bromo-2-oxopropyl)-6-chloroquinazolin-4(3H)-one (38). To a solution of **37** (460 mg, 1.94 mmol) in acetic acid (10 mL) was added bromine (125 μL, 62.42 mmol) dropwise, forming a deep red solution. The reaction mixture was refluxed at 65 °C for 16 h, forming a red precipitate. The reaction mixture was concentrated *in vacuo*, diluted with water and neutralised with 2 M NaOH. The organic layer was extracted with ethyl acetate (3 × 20 mL) and washed with water (2 × 20 mL) and brine (1 × 20 mL). The organic layers were combined and concentrated *in vacuo* and purified through flash column chromatography (1:1 ethyl acetate/petroleum ether), yielding **38** (790 mg, 66%) as a white solid: ^{1}H NMR (DMSO-d_6, 400 MHz) δ 8.27 (s, 1H), 8.08 (d, $J = 2.36$ Hz, 1H), 7.90 (dd, $J = 8.69$, 2.40 Hz, 1H), 7.75 (d, $J = 8.73$ Hz, 1H), 5.13 (s, 2H), 4.57 (s, 2H) ppm; ^{13}C NMR (CDCl$_3$, 101 MHz) δ 194.6, 160.0, 146,7, 146.1, 135.2, 133.6, 129.5, 126.1, 122.8, 52.4, 31.4 ppm; LC-MS (+ESI) calculated for $C_{11}H_8BrClN_2O_2$ *m/z* 314.9 (M + H), found *m/z* 315.1 (M + H).

*4.1.2.13. 2-Isopropylthiazole-5-carbaldehyde oxime (**39**).* Bromomalonaldehyde (150 mg, 1.00 mmol) and 2-methylpro panethioamide (103 mg, 1.00 mmol) were dissolved in EtOH (5 mL) and stirred at room temperature for 4 h. Hydroxylamine hydrochloride (90 mg, 1.30 mmol) and TEA (1 mL) was added and stirred for a further 2 h at room temperature. The reaction mixture was concentrated *in vacuo* and purified through flash column chromatography in petroleum ether/ethyl acetate (4:1 to 3:2) yielding **39** (70 mg, 34%) as a yellow solid: ^{1}H NMR (DMSO-d_6, 400 MHz) δ 12.29 (s, 1H), 8.28 (s, 1H), 8.02−8.00 (m, 3H), 7.54−7.50 (m, 3H) ppm;

*4.1.2.14. (2-Isopropylthiazol-5-yl)methanamine (**40**).* To a solution of **39** (59 mg, 0.29 mmol) in EtOH (4 mL) was added zinc powder (47 mg, 0.72 mmol) and hydrochloric acid (130 μL, 13 N, 1.72 mmol). The reaction mixture was stirred at 60 °C for 2 h, then cooled to room temperature. The mixture was diluted with water and neutralised with saturated NaHCO$_3$, then extracted with ethyl acetate (3 × 15 mL). The combined organic layers were dried over brine and concentrated *in vacuo* yielding **40** (55 mg, 100%) as a yellow solid: ^{1}H NMR (DMSO-d_6, 400 MHz) δ 7.92−7.90 (m, 2H), 7.79 (1H, s), 7.53−7.47 (m, 3H), 5.02 (s, br, 2H), 4.10 (s, 2H) ppm;

*4.1.2.15. Methyl 5-chloro-2-(((dimethylamino)methylene)amino) benzoate (**41**).* A solution of 2-amino-5-chlorobenzoic acid (50 mg, 0.29 mmol) in acetonitrile (5 mL) was treated with 1,1-dimethoxy-*N,N*- dimethylmethanamine and stirred at 100 °C for 2 h. The intermediate **41** was confirmed through LC-MS and carried through without purification: LC-MS (+ESI) calculated for C$_{11}$H$_{13}$ClN$_2$O$_2$ *m/z* 241.1 (M + H), found *m/z* 240.7 (M + H).

*4.1.2.16. 7-Chloroquinazolin-4(3H)-one (**42**).* 4-chloroanthranilic acid (1.00 g, 5.82 mmol) was refluxed in formamide (10 mL) at 150 °C for 16 h, forming a brown precipitate. The reaction mixture was cooled to room temperature and 20 g ice was added. The mixture was left to stand for 1 h, then the precipitate filtered and concentrated *in vacuo*, yielding **42** (850 mg, 81%) as a brown solid: ^{1}H NMR (DMSO-d_6, 400 MHz) δ 12.39 (s, 1H), 8.14 (s, 1H), 8.11 (d, J = 8.56 Hz, 1H), 7.72 (d, J = 2.09 Hz, 1H), 7.55 (dd, J = 8.52, 2.11 Hz, 1H) ppm; ^{13}C NMR (DMSO-d_6, 101 MHz) δ 160.1, 149.9, 146.9, 138.9, 128.0, 127.0, 126.4, 121.5 ppm; LC-MS (+ESI) calculated for C$_8$H$_5$ClN$_2$O *m/z* 181.0 (M + H), found *m/z* 181.2 (M + H).

*4.1.2.17. 7-Chloro-3-(2-oxopropyl)quinazolin-4(3H)-one (**43**).* Compound **42** (850 mg, 4.70 mmol) was dissolved in NMP (5 mL) and treated with NaH (380 mg, 9.40 mmol). The reaction mixture was stirred at room temperature for 30 min, then chloroacetone (1.1 mL, 14.10 mmol) was added dropwise. The reaction was stirred for 30 min at room temperature, the diluted with water (20 mL), and extracted with ethyl acetate (4 × 15 mL). The combined organic layers were dried over brine, concentrated *in vacuo* and recrystallised in 2:1 hexane/ethyl acetate, yielding compound **43** (827 mg, 74%) as a silver crystal: ^{1}H NMR (CDCl$_3$, 400 MHz) δ 8.21 (d, J = 8.52 Hz, 1H), 7.88 (s, 1H), 7.73 (d, J = 2.02 Hz, 1H), 7.47 (dd, J = 8.57, 1.98 Hz, 1H), 4.79 (s, 2H), 2.35 (s, 3H) ppm; ^{13}C NMR (CDCl$_3$, 101 MHz) δ 199.8, 160.4, 149.3, 147.5, 141.0, 128.4, 127.4, 120.5, 77.2, 76.8, 54.8, 27.7 ppm; LC-MS (+ESI) calculated for C$_{11}$H$_9$ClN$_2$O$_2$ *m/z* 237.0 (M + H), found *m/z* 237.1 (M + H).

*4.1.2.18. 7-Chloro-3-(3-chloro-2-oxopropyl)quinazolin-4(3H)-one (**44**).* Compound **43** (235 mg, 1.00 mmol) and NCS (133 mg, 1.00 mmol) were stirred in DCM (5 mL) and H$_2$SO$_4$ (1 mL) at 40 °C for 6 h. The reaction mixture was cooled to room temperature, neutralised with NaOH and extracted with ethyl acetate

(3 × 20 mL). The combined organic layers were dried over brine, concentrated *in vacuo* and purified through flash column chromatography in petroleum ether/ethyl acetate (7:3 to 3:7) yielding **44** as a white solid (30 mg, 11%): ^{1}H NMR (400 MHz, Acetic Acid-d_4) δ 8.43 (s,1H), 8.26 (d, J = 8.59 Hz, 1H), 7.81 (d, J = 2.05 Hz, 1H), 7.59 (dd, J = 8.63, 2.01 Hz, 1H), 5.23 (s, 2H), 4.52 (s, 2H) ppm; ^{13}C NMR (101 MHz, Acetic Acid-d_4) δ 195.7, 160.4, 149.8, 147.7, 141.2, 128.5, 128.4, 125.5, 119.8, 52.7, 46.4 ppm; LC-MS (+ESI) calculated for C$_{11}$H$_8$Cl$_2$N$_2$O$_2$ *m/z* 271.0 (M + H), found *m/z* 270.6 (M + H).

4.2. PqsR bioreporter assay

4.2.1. Bacterial growth conditions

P. aeruginosa strains PAO1-L and PA14 were grown in lysogeny broth (LB). All strains were incubated at 37 °C for 16 h, prior to use when OD$_{600}$ was approximately 2.5. Strains PAO1-L and PA14 contained a chromosomal mCTX:*P$_{pqsA}$-lux* fusion such that light is emitted following activation of the *pqsA* promoter. Consequently, a reduction in bioluminescence is indicative of *pqs* system inhibition. Strain BL21 (DE3) contained a pET28:PqsR plasmid, allowing for overexpression of the protein PqsR, and containing a kanamycin resistance cassette. To these cultures was added 100 μg/mL kanamycin for selection.

4.2.2. Bioluminescence reporter gene IC$_{50}$ and 10 μM spot test assays

Two 1.5 mL Eppendorf tubes were filled with 500 μL of LB broth. To one was added 3.16 μL of a 10 mM stock of a given inhibitor, and to the other 1 μL, resulting in overall concentrations of 63.2 μM and 20 μM respectively. A one in 10 serial dilution of both stock solutions into four further Eppendorf tubes each containing 450 μL of LB broth gave 10 concentrations of the compound from 63.2 μM to 2 nM. Using only the central 60 wells of a Grenier 96 well flat black plate, 100 μL of each concentration was added to three wells for results in triplicate.

Concurrently, an overnight culture of either PAO1-L or PA14 with the relevant antibiotic, grown to an OD$_{600}$ of between 2.0 and 3.0, was diluted in LB broth to OD$_{600}$ = 0.02. To each of the wells containing a given concentration of compound in LB, was added 100 μL of the diluted *P. aeruginosa*, giving overall concentrations of 31.6 μM to 1 nM. The outer wells were filled with 200 μL of LB broth, as well as any unfilled inner wells, and the plate placed into a luminometer-spectrometer (Tecan GENios Pro), running a script at 37 °C over 24 h, with a kinetic cycle measuring OD$_{600}$ and luminescence every 30 min.

A peak in luminescence was observed always between 8 and 9 h, after which deterioration of the growth curve led to a drop in bioluminescence. As such, readouts of the OD$_{600}$ and bioluminescence were taken from the highpoint of the luminescence readout, and the results plotted in Graphpad Prism 8, measuring log [concentration] against luminescence (Relative Light Units)/OD$_{600}$.

A similar methodology was applied for the 10 μM spot test assays, but all compounds were diluted to 10 μM from the 10 mM stock by adding 1 μL of the stock to 500 μL of LB broth, yielding a 20 μM solution. As with the IC$_{50}$ assays, 100 μL was then added to at least three wells and diluted twofold by the addition of 100 μL of *P. aeruginosa* at OD$_{600}$ = 0.02. As all compounds were tested at 10 μM, no serial dilutions of the stock solutions were performed. Data was displayed as a column graph, with all results normalised against the negative control containing 0.1% DMSO (100%).

4.2.3. Crystallography and protein determination

Protein was prepared as previously described by Ilangovan et al. [32] Crystals were grown in 24 well sitting and hanging drop Cryschem plates. Crystallisation reservoir consisted of 100 mM

trisodium citrate, 200 mM ammonium acetate and 2-methyl-2,4-pentanediol (MPD). Citrate pH (5.5−6.5) and MPD concentration (3%−10%) were varied along the plate's X and Y axes respectively, and optimal conditions for crystal soaking of **6**, **12**, **18** and **19** were found to be a pH of 6.25 containing 6% MPD. Ligands were dissolved in DMSO or a multi-component solvent mixture and allowed to incubate in the crystallisation drop for 24 h.

Diffraction images were integrated with DIALS [47] (*via* Xia2 or DUI) and scaled in the CCP4 suite. Structures were solved by Molecular Replacement with PHASER [48] using 6Q7W as a search model. Model was refined with REFAC5 [49] with Jellybody restrains and ligand fitted into the Fo-Fc density map using COOT [50]. Ligand restrains were generated in AceDrg [51]. Omit and POLDER maps were generated using Phenix [52]. Finished structures have been deposited in the PDB as 6Z17 (**6**), 6Z07 (**12**), 6Z5K (**18**) and 6YZ3 (**19**). Ligand description (CIF), is available in supplementary information.

The construct pET28a:pqsR is available upon request.

4.2.4. Pyocyanin quantification

A 5 mL liquid culture of PAO1-L wildtype in LB medium was grown overnight for over 16 h with shaking at 200 rpm. Flasks containing 15 mL overnight PAO1-L culture diluted in LB to an OD_{600} of 0.05, and either an inhibitor compound at $3 \times IC_{50}$ value, or an equivalent volume of DMSO control was added and incubated for a further 16 h with shaking at 200 rpm.

An OD_{600} measurement was taken for each culture after 16 h for normalisation, before each sample was centrifuged for 10 min at $10,000 \times g$ and 24 °C. The supernatants were filtered through a 0.22 μm filter, and 7.5 mL collected. To each 7.5 mL filtered supernatant was added 4.5 mL chloroform, and each sample vortexed at 3000 rpm for 10 s. The samples were centrifuged at 10,000 rcf for 10 min at 4 °C, and the aqueous layer discarded. To 3 mL of each sample was added to 1.5 mL 0.2 M HCl and each vortexed for 10 s, followed by centrifugation at $10,000 \times g$ for 2 min at 4 °C. Measurement of the OD_{520} of the aqueous layer of each sample against a 0.2 M HCl control provided the raw data which could subsequently be normalised against the OD_{600} readings taken after incubation. Adapted from Essar et al. [53].

4.2.5. Cytotoxicity

A549 lung epithelial cells were cultured in Gibco's DMEM media containing 10% FBS and 1% penicillin-streptomycin at 37 °C with 5% CO_2. When 80% confluent, the medium was removed and the cells washed with 2×10 mL PBS and 1×7 mL trypsin-EDTA. To the flask was added 7 mL trypsin-EDTA and incubated for 5 min at 37 °C, 5% CO_2. 7 mL FBS was added to quench trypsinization, and the cells centrifuged at 300 g for 5 min.

The supernatant was removed and the cell pellet washed with DMEM-F12 medium and centrifuged again at 300 g for 5 min. The pellet was then resuspended in 3 mL DMEM-F12 media and diluted further to allow loading of 100 μL of suspension containing 10,000 cells per well into 96 well plates. Cells were incubated for 16 h, at which point 100 μL of each compound was added to the relevant wells to give a total volume of 200 μL. Cells were incubated for a further 16 h, and 20 μL of Alamar blue added to each well. After 5 h incubation, fluorescence was measured with excitation at 510 nm and emission at 590 nm. Values were then normalised against the untreated cell control. Adapted from O'Brien et al. [54].

Author contributions

SG wrote the manuscript with supervision from MS, MC and PW with input from all co-authors. The junior authors performed the experiments and analysed the data with supervision from MS, MC

and PW. FS, MS, MC, PW and JE contributed to the study and experimental design. (Synthesis: SG, FS; Biological Assays: SG and FS; X-ray crystallography WR with supervision from JE.)

Declaration of competing interest

The authors declare that they have no known competing financial interests or personal relationships that could have appeared to influence the work reported in this paper.

Appendix A. Supplementary data

Supplementary data to this article can be found online at https://doi.org/10.1016/j.ejmech.2020.112778.

Abbreviations

AI	auto inducer
AQ	alkyl quinolone
DCM	dichloromethane
DMEM	Dulbecco's modified eagle medium
DMFDMA	*N,N*-dimethylformamide dimethyl acetate
DMSO	dimethyl sulfoxide
EDTA	ethylenediaminetetraacetic acid
EtOH	ethanol
FBS	foetal bovine serum
HHQ	2-heptyl-4-hydroxyquinoline
HPLC	high performance liquid chromatography
IC_{50}	half maximal inhibitory concentration
IPTG	isopropyl β-D-1-thiogalactopyranoside
LB	lysogeny broth
LBD	ligand-binding domain
LC-MS	liquid chromatography-mass spectrometry
LD_{50}	half maximal lethal dose
MCCC	managed chemical compound collection
MPD	2-methyl-2,4-pentanediol
NBS	*N*-bromosuccinimide
NCS	*N*-chlorosuccinimide
NHQ	2-nonyl-4-hydroxyquinoline
NMP	*N*-methyl pyrrolidinone
NMR	nuclear magnetic resonance
OD_{600}	optical density at 600 nm
PA	*Pseudomonas aeruginosa*
PQS	2-heptyl-3-hydroxy-4(1*H*)-quinolone
QS	quorum sensing
QSSM	quorum sensing signal molecule
rcf	relative centrifugal force
SAR	structure-activity relationship
SD	standard deviation
SDS-PAGE	sodium dodecyl sulfate-polyacrylamide gel electrophoresis
TBAI	tetrabutylammonium iodide

TEA   triethylamine
THF   tetrahydrofuran
tris   tris(hydroxymethyl)aminomethane

References

[1] R.L. Henry, C.M. Mellis, L. Petrovic, Mucoid *Pseudomonas aeruginosa* is a marker of poor survival in cystic fibrosis, Pediatr. Pulmonol. 12 (1992) 158−161.

[2] B. Coburn, P.W. Wang, J. Diaz Caballero, S.T. Clark, V. Brahma, S. Donaldson, Y. Zhang, A. Surendra, Y. Gong, D. Elizabeth Tullis, Y.C.W. Yau, V.J. Waters, D.M. Hwang, D.S. Guttman, Lung microbiota across age and disease stage in cystic fibrosis, Sci. Rep. 5 (2015) 10241.

[3] J. Emerson, M. Rosenfeld, S. McNamara, B. Ramsey, R.L. Gibson, *Pseudomonas aeruginosa* and other predictors of mortality and morbidity in young children with cystic fibrosis, Pediatr. Pulmonol. 34 (2002) 91−100.

[4] E. Tacconelli, E. Carrara, A. Savoldi, S. Harbarth, M. Mendelson, D.L. Monnet, C. Pulcini, G. Kahlmeter, J. Kluytmans, Y. Carmeli, M. Ouellette, K. Outterson, J. Patel, M. Cavaleri, E.M. Cox, C.R. Houchens, M.L. Grayson, P. Hansen, N. Singh, U. Theuretzbacher, N. Magrini, WHO pathogens priority list working group. Discovery, research, and development of new antibiotics: the WHO priority list of antibiotic-resistant bacteria and tuberculosis, Lancet Infect. Dis. 18 (2018) 318−327.

[5] A.E. Clatworthy, E. Pierson, D.T. Hung, Targeting virulence: a new paradigm for antimicrobial therapy, Nat. Chem. Biol. 3 (2007) 541−548.

[6] S. Wagner, R. Sommer, S. Hinsberger, C. Lu, R.W. Hartmann, M. Empting, A. Titz, Novel strategies for the treatment of *Pseudomonas aeruginosa* infections, J. Med. Chem. 59 (2016) 5929−5969.

[7] F. Soukarieh, P. Williams, M.J. Stocks, M. Cámara, *Pseudomonas aeruginosa* quorum sensing systems as drug discovery targets: current position and future perspectives, J. Med. Chem. 61 (2018) 10385−10402.

[8] P. Williams, Strategies for inhibiting quorum sensing, Emerg. Top. Life Sci. 1 (2017) 23−30.

[9] M.N. Hurley, M. Cámara, A.R. Smyth, Novel approaches to the treatment of *Pseudomonas aeruginosa* infections in cystic fibrosis, Eur. Respir. J. 40 (2012) 1014−1023.

[10] P. Williams, M. Cámara, Quorum sensing and environmental adaptation in *Pseudomonas aeruginosa*: a tale of regulatory networks and multifunctional signal molecules, Curr. Opin. Microbiol. 12 (2009) 182−191.

[11] S.P. Diggle, K. Winzer, S.R. Chhabra, K.E. Worrall, M. Cámara, P. Williams, The *Pseudomonas aeruginosa* quinolone signal molecule overcomes the cell density-dependency of the quorum sensing hierarchy, regulates *rhl*-dependent genes at the onset of stationary phase and can Be produced in the absence of LasR, Mol. Microbiol. 50 (2003) 29−43.

[12] C. Grandclément, M. Tannières, S. Moréra, Y. Dessaux, D. Faure, Quorum quenching: role in nature and applied developments, FEMS Microbiol. Rev. 40 (2016) 86−116.

[13] R.P. Ryan, J.M. Dow, Diffusible signals and interspecies communication in bacteria, Microbiology (Read.) 154 (2008) 1845−1858.

[14] P. Albuquerque, A. Casadevall, Quorum sensing in fungi–a review, Med. Mycol. 50 (2012) 337−345.

[15] H. Nazik, G. Sass, S.R. Ansari, R. Ertekin, H. Haas, E. Déziel, D.A. Stevens, Novel Intermicrobial Molecular Interaction: *Pseudomonas Aeruginosa* Quinolone Signal (PQS) Modulates *Aspergillus Fumigatus* Response to Iron, 2019. Microbiology (Reading, Engl.).

[16] G.W. Lau, D.J. Hassett, H. Ran, F. Kong, The role of pyocyanin in *Pseudomonas aeruginosa* infection, Trends Mol. Med. 10 (2004) 599−606.

[17] G.W. Lau, H. Ran, F. Kong, D.J. Hassett, D. Mavrodi, *Pseudomonas aeruginosa* pyocyanin is critical for lung infection in mice, Infect. Immun. 72 (2004) 4275−4278.

[18] B.E. Britigan, T.L. Roeder, G.T. Rasmussen, D.M. Shasby, M.L. McCormick, C.D. Cox, Interaction of the *Pseudomonas aeruginosa* secretory products pyocyanin and pyochelin generates hydroxyl radical and causes synergistic damage to endothelial cells. Implications for *Pseudomonas*-associated tissue injury, J. Clin. Invest. 90 (1992) 2187−2196.

[19] A. Stintzi, K. Evans, J.-M. Meyer, K. Poole, Quorum sensing and siderophore biosynthesis in *Pseudomonas aeruginosa*: LasR/LasI mutants exhibit reduced pyoverdine biosynthesis, FEMS Microbiol. Lett. 166 (1998) 341−345.

[20] A. Glessner, R.S. Smith, B.H. Iglewski, J.B. Robinson, Roles of *Pseudomonas aeruginosa las* and *rhl* quorum-sensing systems in control of twitching motility, J. Bacteriol. 181 (1999) 1623−1629.

[21] C. Reimmann, N. Ginet, L. Michel, C. Keel, P. Michaux, V. Krishnapillai, M. Zala, K. Heurlier, K. Triandafillu, H. Harms, G. Défago, D. Haas, Genetically programmed autoinducer destruction reduces virulence gene expression and swarming motility in *Pseudomonas aeruginosa* PAO1, Microbiology (Read.) 148 (2002) 923−932.

[22] C.T. O'Loughlin, L.C. Miller, A. Siryaporn, K. Drescher, M.F. Semmelhack, B.L. Bassler, A quorum-sensing inhibitor blocks *Pseudomonas aeruginosa* virulence and biofilm formation, Proc. Natl. Acad. Sci. U.S.A. 110 (2013) 17981−17986.

[23] J. Lee, L. Zhang, The hierarchy quorum sensing network in *Pseudomonas aeruginosa*, Protein Cell 6 (2015) 26−41.

[24] G. Rampioni, L. Leoni, P. Williams, The art of antibacterial warfare: deception through interference with quorum sensing-mediated communication, Bioorg. Chem. 55 (2014) 60−68.

[25] S. Heeb, M.P. Fletcher, S.R. Chhabra, S.P. Diggle, P. Williams, M. Cámara, Quinolones: from antibiotics to autoinducers, FEMS Microbiol. Rev. 35 (2011) 247−274.

[26] S.L. Drees, S. Fetzner, PqsE of *Pseudomonas aeruginosa* acts as pathway-specific thioesterase in the biosynthesis of alkylquinolone signaling molecules, Chem. Biol. 22 (2015) 611−618.

[27] J.P. Coleman, L.L. Hudson, S.L. McKnight, J.M. Farrow, M.W. Calfee, C.A. Lindsey, E.C. Pesci, *Pseudomonas aeruginosa* PqsA is an anthranilate-coenzyme A ligase, J. Bacteriol. 190 (2008) 1247−1255.

[28] S.L. Drees, C. Li, F. Prasetya, M. Saleem, I. Dreveny, P. Williams, U. Hennecke, J. Emsley, S. Fetzner, PqsBC, a condensing enzyme in the biosynthesis of the *Pseudomonas aeruginosa* quinolone signal: crystal structure, inhibition, and reaction mechanism, J. Biol. Chem. 291 (2016) 6610−6624.

[29] J.H. Sahner, M. Empting, A. Kamal, E. Weidel, M. Groh, C. Börger, R.W. Hartmann, Exploring the chemical space of ureidothiophene-2-carboxylic acids as inhibitors of the quorum sensing enzyme PqsD from *Pseudomonas aeruginosa*, Eur. J. Med. Chem. 96 (2015) 14−21.

[30] D. Pistorius, A. Ullrich, S. Lucas, R.W. Hartmann, U. Kazmaier, R. Müller, Biosynthesis of 2-alkyl-4(1H)-Quinolones in Pseudomonas aeruginosa: potential for therapeutic interference with pathogenicity, Chembiochem 12 (2011) 850−853.

[31] Y.-C. Liu, F. Hussain, O. Negm, A. Pavia, N. Halliday, J.-F. Dubern, S. Singh, S. Muntaka, L. Wheldon, J. Luckett, P. Tighe, C. Bosquillon, P. Williams, M. Cámara, L. Martínez-Pomares, Contribution of the alkylquinolone quorum-sensing system to the interaction of *Pseudomonas aeruginosa* with bronchial epithelial cells, Front. Microbiol. 9 (2018) 3018.

[32] A. Ilangovan, M. Fletcher, G. Rampioni, C. Pustelny, K. Rumbaugh, S. Heeb, M. Cámara, A. Truman, S.R. Chhabra, J. Emsley, P. Williams, Structural basis for native agonist and synthetic inhibitor recognition by the *Pseudomonas aeruginosa* quorum sensing regulator PqsR (MvfR), PLoS Pathog. 9 (2013) e1003508.

[33] C. Lu, B. Kirsch, C. Zimmer, J.C. de Jong, C. Henn, C.K. Maurer, M. Müsken, S. Häussler, A. Steinbach, R.W. Hartmann, Discovery of antagonists of PqsR, a key player in 2-alkyl-4-quinolone-dependent quorum sensing in *Pseudomonas aeruginosa*, Chem. Biol. 19 (2012) 381−390.

[34] F. Soukarieh, E. Vico Oton, J.F. Dubern, J. Gomes, N. Halliday, M. de Pilar Crespo, J. Ramírez-Prada, B. Insuasty, R. Abonia, J. Quiroga, S. Heeb, P. Williams, M.J. Stocks, M. Cámara, *In silico* and *in vitro*-guided identification of inhibitors of alkylquinolone-dependent quorum sensing in *Pseudomonas aeruginosa*, Molecules 23 (2018) 257.

[35] M. Chatterjee, S. D'Morris, V. Paul, S. Warrier, A.K. Vasudevan, M. Vanuopadath, S.S. Nair, B. Paul-Prasanth, C.G. Mohan, R. Biswas, Mechanistic understanding of phenyllactic acid mediated inhibition of quorum sensing and biofilm development in *Pseudomonas aeruginosa*, Appl. Microbiol. Biotechnol. 101 (2017) 8223−8236.

[36] T. Kitao, F. Lepine, S. Babloudi, F. Walte, S. Steinbacher, K. Maskos, M. Blaesse, M. Negri, M. Pucci, B. Zahler, A. Felici, L.G. Rahme, Molecular insights into function and competitive inhibition of *Pseudomonas aeruginosa* multiple virulence factor regulator, mBio 9 (2018).

[37] M. Starkey, F. Lepine, D. Maura, A. Bandyopadhaya, B. Lesic, J. He, T. Kitao, V. Righi, S. Milot, A. Tzika, L. Rahme, Identification of anti-virulence compounds that disrupt quorum-sensing regulated acute and persistent pathogenicity, PLoS Pathog. 10 (2014), e1004321.

[38] J.T. Gupton, J.F. Miller, R.D. Bryant, P.R. Maloney, B.S. Foster, The preparation of aromatic amidino esters and their reaction with primary amines, Tetrahedron 43 (1987) 1747−1752.

[39] M.P. Fletcher, S.P. Diggle, S.A. Crusz, S.R. Chhabra, M. Cámara, P. Williams, A dual biosensor for 2-alkyl-4-quinolone quorum-sensing signal molecules, Environ. Microbiol. 9 (2007) 2683−2693.

[40] T. Köhler, M. Michea-Hamzehpour, P. Plesiat, A.L. Kahr, J.C. Pechere, Differential selection of multidrug efflux systems by quinolones in *Pseudomonas aeruginosa*, Antimicrob. Agents Chemother. 41 (1997) 2540−2543.

[41] V.N. Viswanadhan, A.K. Ghose, G.R. Revankar, R.K. Robins, Atomic physicochemical parameters for three dimensional structure directed quantitative structure-activity relationships. 4. Additional parameters for hydrophobic and dispersive interactions and their application for an automated superposition of certain naturally occurring nucleoside antibiotics, J. Chem. Inf. Model. 29 (1989) 163−172.

[42] I. Aleksić, S. Šegan, F. Andrić, M. Zlatović, I. Moric, D.M. Opsenica, L. Senerovic, Long-chain 4-aminoquinolines as quorum sensing inhibitors in *Serratia marcescens* and *Pseudomonas aeruginosa*, ACS Chem. Biol. 12 (2017) 1425−1434.

[43] H. Mikkelsen, R. McMullan, A. Filloux, The *Pseudomonas aeruginosa* reference strain PA14 displays increased virulence due to a mutation in LadS, PLoS One 6 (2011), e29113.

[44] M. Zender, F. Witzgall, A. Kiefer, B. Kirsch, C.K. Maurer, A.M. Kany, N. Xu, S. Schmelz, C. Börger, W. Blankenfeldt, M. Empting, Flexible fragment growing boosts potency of quorum-sensing inhibitors against *Pseudomonas aeruginosa* virulence, ChemMedChem 15 (2020) 188−194.

[45] I. Aleksic, J. Jeremic, D. Milivojevic, T. Ilic-Tomic, S. Šegan, M. Zlatović, D.M. Opsenica, L. Senerovic, N-benzyl derivatives of long-chained 4-amino-7-chloro-quionlines as inhibitors of pyocyanin production in *Pseudomonas aeruginosa*, ACS Chem. Biol. 14 (2019) 2800−2809.

[46] M.A. Hossain, N. Sattenapally, H.I. Parikh, W. Li, K.P. Rumbaugh, N.A. German,

Design, synthesis, and evaluation of compounds capable of reducing *Pseudomonas aeruginosa* virulence, Eur. J. Med. Chem. 185 (2020) 111800.

[47] G. Winter, D.G. Waterman, J.M. Parkhurst, A.S. Brewster, R.J. Gildea, M. Gerstel, L. Fuentes-Montero, M. Vollmar, T. Michels-Clark, I.D. Young, N.K. Sauter, G. Evans, DIALS: implementation and evaluation of a new integration package, Acta Crystallogr. D Struct. Biol. 74 (2018) 85–97.

[48] A.J. McCoy, R.W. Grosse-Kunstleve, P.D. Adams, M.D. Winn, L.C. Storoni, R.J. Read, Phaser crystallographic software, J. Appl. Crystallogr. 40 (2007) 658–674.

[49] O. Kovalevskiy, R.A. Nicholls, F. Long, A. Carlon, G.N. Murshudov, Overview of refinement procedures within REFMAC5: utilizing data from different sources, Acta Crystallogr. D Struct. Biol. 74 (2018) 215–227.

[50] P. Emsley, B. Lohkamp, W.G. Scott, K. Cowtan, Features and development of coot, Acta Crystallogr. Sect. D Biol. Crystallogr. 66 (2010) 486–501.

[51] F. Long, R.A. Nicholls, P. Emsley, S. Graæulis, A. Merkys, A. Vaitkus, G.N. Murshudov, AceDRG: a stereochemical description generator for ligands, Acta Crystallogr. D Struct. Biol. 73 (2017) 112–122.

[52] D. Liebschner, P.V. Afonine, N.W. Moriarty, B.K. Poon, O.V. Sobolev, T.C. Terwilliger, P.D. Adams, Polder maps: improving OMIT maps by excluding bulk solvent, Acta Crystallogr. D Struct. Biol. 73 (2017) 148–157.

[53] D.W. Essar, L. Eberly, A. Hadero, I.P. Crawford, Identification and characterization of genes for a second anthranilate synthase in *Pseudomonas aeruginosa*: interchangeability of the two anthranilate synthases and evolutionary implications, J. Bacteriol. 172 (1990) 884–900.

[54] J. O'Brien, I. Wilson, T. Orton, F. Pognan, Investigation of the alamar blue (resazurin) fluorescent dye for the assessment of mammalian cell cytotoxicity, Eur. J. Biochem. 267 (2000) 5421–5426.